



UNIVERSITI PUTRA MALAYSIA

***EFFECTS OF SINTERING TEMPERATURE ON THERMAL,
MECHANICAL AND DIELECTRIC PROPERTIES OF SiC/Si₃N₄
NANOPARTICLES-INSERTED KAOLINITE–MULLITE***

ALEX SEE

ITMA 2016 9



**EFFECTS OF SINTERING TEMPERATURE ON THERMAL,
MECHANICAL AND DIELECTRIC PROPERTIES OF SiC/Si₃N₄
NANOPARTICLES-INSERTED KAOLINITE–MULLITE**

By

ALEX SEE

**Thesis Submitted to the School of Graduate Studies, Universiti Putra Malaysia,
in Fulfillment of the Requirements for the Degree of Doctor of Philosophy**

March 2016

COPYRIGHT

All materials contained within the thesis, including without limitation, text, logos, icons, photographs and all other works is copyright material of Universiti Putra Malaysia unless otherwise stated. Use may be made of any material contained within the thesis for non-commercial purposes from the copyright holder. Commercial use of the material may only be made with the express, prior permission of Universiti Putra Malaysia.

Copyright© Universiti Putra Malaysia.



DEDICATION

In memory of Associate Professor Dr Mansor Hashim,

Who taught me there is a purpose behind every material, no matter whether the material exhibits good or bad physical properties.

“Engineering is quite different from science. Scientists try to understand nature. Engineers try to make things that do not exist in nature. Engineers stress invention. To embody an invention the engineer must put his idea in concrete terms, and design something that people can use. That something can be a device, a gadget, a material, a method, a computing program, an innovative experiment, a new solution to a problem, or an improvement on what is existing. Since a design has to be concrete, it must have its geometry, dimensions, and characteristic numbers. Almost all engineers working on new designs find that they do not have all the needed information. Most often, they are limited by insufficient scientific knowledge. Thus they study mathematics, physics, chemistry, biology and mechanics. Often they have to add to the sciences relevant to their profession. Thus engineering sciences are born.”

Yung Cheng Fung, Classical and Computational Mechanics, (2001)

Abstract of thesis presented to the Senate of Universiti Putra Malaysia in fulfillment of requirement for the degree of Doctor of Philosophy

**EFFECTS OF SINTERING TEMPERATURE ON THERMAL,
MECHANICAL AND DIELECTRIC PROPERTIES OF SiC/Si₃N₄
NANOPARTICLES-INSERTED KAOLINITE –MULLITE**

By

ALEX SEE

March 2016

Chairman: Associate Professor Jumiah Hassan, PhD
Faculty : Institute of Advanced Technology

Malaysian kaolinite production and exports have declined despite increasing global consumption of kaolinite material in paper and whiteware industries. New applications for Malaysian kaolinite are necessary to improve its competitiveness in the global environment. This research was designed to test the hypothesis that insertion of nanoparticles within a micron grain-size matrix will form a composite material with enhanced values in thermal, mechanical and electrical properties. The matrix chosen was a kaolinite-mullite matrix and the nanoparticles selected were β -Silicon Carbide (SiC) and amorphous Silicon Nitride (SN). Both Silicon Carbide-Mullite (SC-M) and Silicon Nitride-Mullite (SN-M) composite powders were prepared with a mixed solution followed by conventional sintering in an argon environment at 1000 °C, 1100 °C and 1200 °C temperatures.

XRD data of the SC-M composites yielded kaolinite-mullite products with embedded SiC presence. The SN-M composites however, yield the presence of α - and β -Silicon Nitride phases as the amorphous nanoparticles were detected to be crystalline by the XRD data. Densities of the composites were lower than the true density of the mullite matrix as the composites weights were influenced by the bulk densities of the nanopowders. Thermal diffusivity of the SC-M and SN-M composites yielded lower values as compared to the thermal diffusivity of the Kaolinite matrix itself. The thermal diffusivity values of both SC-M and SN-M were dependent on the presence of mullite concentration within the matrix.

Mechanical measurements of the SC-M and SN-M composites yielded significantly higher compressive strength as compared to those of the matrix samples. Kaolinite-mullite samples presented layered fractures under the compression test with a maximum value of 21.3 MPa. The 5% SC-M sample yielded compression strength of 54.2 MPa. SiC additions higher than 5% have lower, linear compression relation with a sharp break at maximum. SN-M composites exhibited typical ceramic compression strength at low weight additions; higher SN additions displayed a constant

compression loading effect followed by ceramic loading behavior with 30% SN-M displaying ultimate compressive strength of 110 MPa.

Dielectric permittivity of the kaolinite-mullite matrix samples has low relaxation behavior with ϵ_r' values marked at 9.3 to 19.3 units (at 1 MHz) for room temperature measurement. The insertion of SiC nanoparticles has elevated the real dielectric permittivity range from 5.7 units to 17.1 at 1 MHz. Insertion of the SN nanoparticles exhibited dielectric suppression as the relative dielectric permittivity values were lower than those of the matrix itself, from 4.1 to 12.2 units at 1 MHz.

The insertion of nanoparticles within the kaolinite-mullite matrix is fruitful as different properties can be examined in detail. Both SiC and SN nanoparticles yielded different degrees of enhancements in thermal, mechanical and electrical properties. The nanoparticles insertions were beneficial to thermal and electrical insulating behavior as well as mechanical compression strength.

Abstrak tesis yang dikemukakan kepada Senat Universiti Putra Malaysia sebagai memenuhi keperluan untuk ijazah Doktor Falsafah

**KESAN SUHU PENSINTERAN KE ATAS SIFAT TERMA, MEKANIKAL
DAN DIELEKTRIK KAOLINIT-MULLITE YANG DISISIPKAN
NANOPARTIKEL SiC/Si₃N₄**

Oleh

ALEX SEE

Mac 2016

Pengerusi: Profesor Madya Jumiah Hassan, PhD

Faculti : Institut Teknologi Maju

Penghasilan dan eksport kaolinit Malaysia telah menurun walaupun terdapat peningkatan dalam penggunaan global dalam industri kertas dan tembikar putih. Aplikasi baru untuk kaolinit Malaysia adalah diperlukan untuk meningkatkan daya saing bahan tersebut dalam persekitaran global. Penyelidikan ini bertujuan untuk menguji hipotesis bahawa penyuntikan nanopartikel dalam butiran matriks bersaiz mikron akan membentuk bahan komposit dengan peningkatan di dalam nilai-nilai sifat terma, mekanikal dan elektrik. Matriks yang terpilih adalah matriks kaolinit-mullite serta nanopartikel yang terpilih ialah β -Silikon Karbida (SiC) dan Silicon Nitrida beramorfus (SN). Kedua-dua serbuk komposit Silikon Karbida-Mullite (SC-M) dan Silikon Nitrida-Mullite (SN-M) telah disediakan dengan larutan campuran diikuti oleh pensinteran konvensional dalam persekitaran argon pada suhu 1000 °C, 1100 °C dan 1200 °C.

Data XRD bagi komposit SC-M telah menunjukkan sifat SiC tebenam dalam produk kaolinit-mullit. Walau bagaimanapun, komposit SN-M menunjukkan kehadiran fasa α - dan β -Silikon Nitrida setelah nanopartikel amorfus dikesan berada dalam keadaan kristal oleh data XRD. Ketumpatan bahan-bahan komposit adalah lebih rendah daripada ketumpatan sebenar matriks mullite kerana berat komposit dipengaruhi oleh ketumpatan pukal serbuk nano. Sifat kemeresapan terma komposit SC-M dan SN-M telah menghasilkan nilai-nilai yang lebih rendah berbanding dengan data kemeresapan terma matriks kaolinit sendiri. Nilai-nilai kemeresapan terma kedua-dua SC-M dan SN-M bergantung kepada kehadiran konsentrasi matriks mullite dalam matriks tersebut.

Kajiuji sifat mekanikal komposit SC-M dan SN-M telah menghasilkan kekuatan mampatan yang lebih tinggi berbanding dengan sifat sampel matriks. Sampel kaolinit-mullite menunjukkan sifat pematahan secara berlapis di bawah ujian mampatan dengan nilai maksimum sebanyak 21.3 MPa. Sampel 5% SC-M menghasilkan kekuatan mampatan sebanyak 54.2 MPa. Penambahan SiC melebihi 5%

mempunyai sifat yang lebih rendah berhubungan dengan mampatan linear serta patahan mendadak pada takat maksimum. Komposit SN-M yang dipamerkan menunjukkan kekuatan mampatan seramik pada konsentrasi SN yang rendah; Penambahan SN yang lebih tinggi memaparkan kesan muatan mampatan yang malar diikuti dengan sifat muatan seramik engan 30% SN-M memaparkan kekuatan mampatan muktamad 110 MPa.

Sifat ketelusan dielektrik sampel matriks kaolinit-mullite mempunyai sifat santaian yang rendah dengan nilai-nilai ϵ_r' di antara 9.3 – 19.3 unit (pada 1 MHz) dalam pengukuran pada suhu bilik. Penyuntikan nanopartikel SiC telah meningkatkan sifat ketelusan dielektrik sebenar daripada 5.7 kepada 17.1 pada 1 MHz. Penyuntikan nanopartikel SN memaparkan sifat penyekatan dielektrik dengan nilai-nilai ketelusan dielektrik relatif yang lebih rendah berbanding sifat matriks itu sendiri, dari 4.1 kepada 12.2 unit pada 1 MHz.

Penyisipan nanopartikel dalam matriks kaolinit-mullite membawa manfaat apabila sifat yang berbeza boleh dikaji secara terperinci. Kedua-dua nanopartikel SiC dan SN telah menghasilkan takat penambahbaikan yang berbeza dalam sifat terma, mekanikal dan elektrik. Penyisipan nanopartikel telah memberi manfaat kepada sifat penebat terma dan elektrik serta kekuatan mampatan mekanikal.

ACKNOWLEDGEMENTS

I would like say thanks to my supervisors, Associate Professor Dr. Jumiah Hassan, the late Associate Professor Dr. Mansor Hashim and Associate Professor Dr. Zaidan Abdul Wahab for their patience and assistance in guiding me throughout the entire research process.

I would also like to thank Associate Professor Dr. Chen Soo Kian and Tan Kwee Yong for their assistance in the Argon environment sintering facilities. I would like to thank also Wong Swee Ying, Tan Foo Khoon, Leow Chun Yan, Wong Yick Jeng, Mutia Suhaibah Abdullah and Dayang Nur Fazaliana Abdul Halim for their help.

I would like to thank the financial assistance offered by the Malaysian Ministry of Higher Education (MOHE) and the MyBrain scholarship program, which has sponsored a major part of this research.

Finally, I would like to thank my father, my mother and family for their financial support and guidance throughout the entire research period. Their understanding and encouragement is essential to the success of this research project.

“Engineering is the art or science of making practical.”

Samuel Charles Florman, The Existential Pleasures of Engineering (1976)

“Science is concerned with what is possible while engineering is concerned with choosing, from among the many possible ways, one that meets a number of often poorly stated economic and practical objectives.”

Richard Hamming, Turing Award lecture (1968), 'One Man's View of Computer Science', collected in ACM Turing Award Lectures: The First Twenty Years, 1966 to 1985 (1987), 209.

I certify that a Thesis Examination Committee has met on 1 March 2016 to conduct the final examination of Alex See on his thesis entitled "Effects of Sintering Temperature on Thermal, Mechanical and Dielectric Properties of SiC/Si₃N₄ Nanoparticles-Inserted Kaolinite-Mullite " in accordance with the Universities and University Colleges Act 1971 and the Constitution of the Universiti Putra Malaysia [P.U.(A) 106] 15 March 1998. The Committee recommends that the student be awarded the Doctor of Philosophy.

Members of the Thesis Examination Committee were as follows:

Hishamuddin bin Zainuddin, PhD

Associate Professor
Faculty of Science
Universiti Putra Malaysia
(Chairman)

Azmi bin Zakaria, PhD

Professor
Faculty of Science
Universiti Putra Malaysia
(Internal Examiner)

Khamirul Amin bin Matori, PhD

Associate Professor
Faculty of Science
Universiti Putra Malaysia
(Internal Examiner)

Gour Prasad Das, PhD

Professor
Indian Association for the Cultivation of Science
India
(External Examiner)



ZULKARNAIN ZAINAL, PhD

Professor and Deputy Dean
School of Graduate Studies
Universiti Putra Malaysia

Date: 25 May 2016

This thesis was submitted to the Senate of Universiti Putra Malaysia and has been accepted as fulfillment of the requirement for the degree of Doctor of Philosophy. The members of the Supervisory Committee were as follows:

Jumiah Hassan, PhD

Associate Professor
Faculty of Science
Universiti Putra Malaysia
(Chairman)

Mansor Hashim, PhD

Associate Professor
Institute of Advanced Technology
Universiti Putra Malaysia
(Member)

Zaidan Abdul Wahab, PhD

Associate Professor
Faculty of Science
Universiti Putra Malaysia
(Member)

BUJANG KIM HUAT, PhD

Professor and Dean
School of Graduate Studies
Universiti Putra Malaysia

Date:

Declaration by graduate student

I hereby confirm that:

- This thesis is my original work;
- Quotations, illustrations and citations have been duly referenced;
- This thesis has not been submitted previously or concurrently for any other degree at any other institutions;
- Intellectual property from the thesis and copyright of the thesis are fully-owned by Universiti Putra Malaysia, as according to the Universiti Putra Malaysia (Research) Rules 2012;
- Written permission must be obtained from the supervisor and the office of Deputy Vice Chancellor (Research and Innovation) before the thesis is published (in the form of written, printed or electronic form) including books, journals, modules, proceedings, popular writings, seminar papers, manuscripts, posters, reports, lectures notes, learning modules or any other materials as stated in the Universiti Putra Malaysia (Research) Rules 2012;
- There is no plagiarism or data falsification/fabrication in the thesis and scholarly integrity was upheld as according to the Universiti Putra Malaysia (Graduate Studies) Rules 2003 (Revision 2012-2013) and the Universiti Putra Malaysia (Research) Rules 2012. The thesis has undergone plagiarism detection software.

Signature: _____ Date: _____

Name and Matric Number: Alex See, GS27384

Declaration by the Members of the Supervisory Committee

This is to confirm that:

- The research conducted and the writing of this thesis was under our supervision;
- Supervision responsibilities as stated in the Universiti Putra Malaysia (Graduate Studies) Rules 2003 (Revision 2012-2013) are adhered to.

Signature: _____

Name of
Chairman of

Supervisory Committee: Associate Professor Dr. Jumiah Hassan

Signature: _____

Name of
Member of

Supervisory Committee: Associate Professor Dr. Mansor Hashim

Signature: _____

Name of
Member of

Supervisory Committee: Associate Professor Dr. Zaidan Abdul Wahab

TABLE OF CONTENTS

	ABSTRACT	Page
	ABSTRAK	i
	ACKNOWLEDGEMENTS	iii
	APPROVAL	v
	DECLARATION	vi
	LIST OF TABLES	viii
	LIST OF FIGURES	xiv
	LIST OF ABBREVIATIONS	xvi
		xxvii
CHAPTER		
1	INTRODUCTION	1
	1.1 Introduction	1
	1.2 Research Background	2
	1.3 Problem Statement	2
	1.4 Matrix Information	3
	1.5 Filler Information	4
	1.5.1 Silicon Carbide	4
	1.5.2 Silicon Nitride	6
	1.6 Theoretical Framework	7
	1.7 Conceptual Framework	8
	1.8 Research Objectives	9
	1.9 Research Limitations	9
2	LITERATURE REVIEW	11
	2.1 Introduction	11
	2.2 Properties of Individual Materials	11
	2.2.1 Thermal Properties of Mullite	11
	2.2.2 Electrical Properties of Mullite	12
	2.2.3 Mechanical Properties of Mullite	13
	2.3 Properties of Silicon Carbide (SiC) Filler Material	14
	2.3.1 Thermal Properties of SiC	14
	2.3.2 Electrical Properties of SiC	15
	2.3.3 Mechanical Properties of SiC	17
	2.4 Properties of Silicon Nitride (SN) Filler Material	18
	2.4.1 Thermal Properties of SN	18
	2.4.2 Electrical Properties of SN	19
	2.4.3 Mechanical Properties of SN	20
	2.5 Thermal Properties of Ceramic Matrix Composites	21
	2.6 Mechanical Properties of Ceramic Matrix Composites	22
	2.7 Electrical and Dielectric Properties of Ceramic Matrix Composites	24
	2.8 Particle Packing and Compaction Mechanisms in Composites	26

3	MATERIALS AND METHODOLOGY	32
3.1	Introduction	32
3.2	Preparation of Silicon Carbide-Mullite (SC-M) Pellet Series and Silicon Nitride-Mullite (SN-M) Pellet Series	32
3.2.1	Weighing	33
3.2.2	Mixing	34
3.2.3	Filtering and Drying	34
3.2.4	Sieving	34
3.2.5	Moulding	35
3.2.6	Final Sintering	35
3.3	Special Preparation for the Composites in Mechanical Compression Tests	36
3.3.1	Introduction	36
3.3.2	Mould Design	36
3.3.3	Moulding Process	38
3.3.4	Sintering	39
3.4	Characterization and Testing Methods	39
3.4.1	X-Ray Diffraction (XRD)	39
3.4.2	FESEM Microscopy	40
3.4.3	Density Measurements	40
3.4.4	Low Frequency Dielectric Measurements	40
3.4.5	Thermal Diffusivity Measurements	41
4	STRUCTURAL AND THERMAL PROPERTIES	45
4.1	Introduction	45
4.2	XRD Spectroscopy	45
4.2.1	XRD Spectroscopy of Mullite Matrix	45
4.2.2	XRD Spectroscopy of Silicon Carbide Mullite (SC-M) Series	47
4.2.3	XRD Spectroscopy of Silicon Nitride Mullite (SN-M) Series	50
4.3	Determination of Density for the Composites	53
4.3.1	Density of Mullite Matrix	53
4.3.2	Density of Silicon Carbide-Mullite Series	54
4.3.3	Density of Silicon Nitride-Mullite Series	58
4.4	Thermal Diffusivity Measurements	62
4.4.1	Thermal Diffusivity of Mullite Matrix	62
4.4.2	Thermal Diffusivity of Silicon Carbide-Mullite Series	64
4.4.3	Thermal Diffusivity of Silicon Nitride-Mullite Series	69
4.5	Enhancement by SiC Nanoparticles	74
4.6	Enhancement by SN Nanoparticles	78
4.7	Conclusions	81

5	MECHANICAL PROPERTIES AND INTERNAL MORPHOLOGY	83
5.1	Introduction	83
5.2	Mechanical Properties of Mullite Matrix	83
5.3	Mechanical Properties of Silicon Carbide-Mullite Series	87
5.4	Mechanical Properties of Silicon Nitride-Mullite Series	105
5.5	Density and UCS to Density Variations of the SC-M Cylinders	123
5.6	Density and UCS to Density Variations of the SN-M Cylinders	126
5.7	Analysis of the Mechanical Behavior of SC-M and SN-M Ceramics	128
5.8	Morphological Examinations of the Mullite Ceramics Before and After the Compression Test	131
5.9	Morphological Examinations of the SC-Mullite Ceramics Before and After the Compression Test	132
5.10	Morphological Examinations of the SN-Mullite Ceramics Before and After the Compression Test	139
5.11	Discussions	146
5.12	Conclusions	149
6	DIELECTRIC PROPERTIES	150
6.1	Introduction	150
6.2	Dielectric properties of Mullite Matrix and Nanoparticle Fillers	150
6.2.1	Pure Mullite Matrix	150
6.2.2	Pure SiC Nanoparticles	155
6.2.3	Pure SN Nanoparticles	156
6.3	Dielectric Properties of SC-M Composites	157
6.3.1	5% SC-M	157
6.3.2	10% SC-M	161
6.3.3	15% SC-M	164
6.3.4	20% SC-M	167
6.3.5	25% SC-M	171
6.3.6	30% SC-M	174
6.4	Dielectric Properties of SN-M Composites	177
6.4.1	5% SN-M	177
6.4.2	10% SN-M	180
6.4.3	15% SN-M	183
6.4.4	20% SN-M	187
6.4.5	25% SN-M	191
6.4.6	30% SN-M	195
6.5	Work Efficiency of the Nanoparticle Enhancement	198
6.5.1	Enhancement by SiC Nanoparticle	198
6.5.2	Enhancement by SN Nanoparticle	205
6.6	Discussion on Enhancement by Nanoparticle Insertion	211
6.7	Conclusions	218

7	RESEARCH CONCLUSIONS	219
7.1	Research Conclusion	219
7.2	Future Research Work	220
7.3	Potential Applications	221
	REFERENCES	222
	APPENDICES	233
	BIODATA OF STUDENT	246
	LIST OF PUBLICATIONS	247



LIST OF TABLES

Table		Page
2.1	Mechanical and Thermal Properties of Mullite [60]	14
2.2	Packing Densities Based on Crystal Arrangement and Coordination Number [104]	27
2.3	Densities Differences from Poured and Tapping Methods Based on Powder Morphology	27
3.1	Composition of SiC Added to Mullite (200 gm batches)	33
3.2	Composition of Si ₃ N ₄ Added to Mullite (200 gm batches)	34
A1	Relative Dielectric Permittivity of the Pure Mullite Matrix, SiC and SN Nanoparticles According To Frequency Response	234
A2	Relative Dielectric Properties of the SC-M Composite Ceramic Series at 40 Hz	235
A3	Relative Dielectric Properties of the SC-M Composite Ceramic Series at 1 KHz	236
A4	Relative Dielectric Properties of the SC-M Composite Ceramic Series at 1 MHz	237
A5	Relative Dielectric Properties of the SN-M Composite Ceramic Series at 40 Hz	238
A6	Relative Dielectric Properties of the SN-M Composite Ceramic Series at 1 KHz	239
A7	Relative Dielectric Properties of the SN-M Composite Ceramic Series at 1 MHz	240
A8	Temperature Effects of Relative Dielectric Permittivity (40 Hz Response) of the SC-M Ceramics Sintered at 1000°C	241
A9	Temperature Effects of Relative Dielectric Permittivity (40 Hz Response) of the SC-M Ceramics Sintered at 1100°C	241
A10	Temperature Effects of Relative Dielectric Permittivity (40 Hz Response) of the SC-M Ceramics Sintered at 1200°C	241
A11	Temperature Effects of Relative Dielectric Permittivity (1 KHz Response) of the SC-M Ceramics Sintered at 1000°C	242
A12	Temperature Effects of Relative Dielectric Permittivity (1 KHz Response) of the SC-M Ceramics Sintered at 1100°C	242
A13	Temperature Effects of Relative Dielectric Permittivity (1 KHz Response) of the SC-M Ceramics Sintered at 1200°C	242
A14	Temperature Effects of Relative Dielectric Permittivity (1 MHz Response) of the SC-M Ceramics Sintered at 1000°C	243
A15	Temperature Effects of Relative Dielectric Permittivity (1 MHz Response) of the SC-M Ceramics Sintered at 1100°C	243
A16	Temperature Effects of Relative Dielectric Permittivity (1 MHz Response) of the SC-M Ceramics Sintered at 1200°C	243

A17	Temperature Effects of Relative Dielectric Permittivity (40 Hz Response) of the SN-M Ceramics Sintered at 1000°C	244
A18	Temperature Effects of Relative Dielectric Permittivity (40 Hz Response) of the SN-M Ceramics Sintered at 1100°C	244
A19	Temperature Effects of Relative Dielectric Permittivity (40 Hz Response) of the SN-M Ceramics Sintered at 1200°C	244
A20	Temperature Effects of Relative Dielectric Permittivity (1 KHz Response) of the SN-M Ceramics Sintered at 1000°C	245
A21	Temperature Effects of Relative Dielectric Permittivity (1 KHz Response) of the SN-M Ceramics Sintered at 1100°C	245
A22	Temperature Effects of Relative Dielectric Permittivity (1 KHz Response) of the SN-M Ceramics Sintered at 1200°C	245
A23	Temperature Effects of Relative Dielectric Permittivity (1 MHz Response) of the SN-M Ceramics Sintered at 1000°C	246
A24	Temperature Effects of Relative Dielectric Permittivity (1 MHz Response) of the SN-M Ceramics Sintered at 1100°C	246
A25	Temperature Effects of Relative Dielectric Permittivity (1 MHz Response) of the SN-M Ceramics Sintered at 1200°C	246

LIST OF FIGURES

Figure	Page
1.1 Global Consumption of Kaolin Clay	2
1.2 Kaolinite and Mullite Crystal Structure [18]	3
1.3 Phase Diagram For the Kaolinite to Mullite Transformation [19]	4
1.4 (a) β -SiC and (b) α -SiC Crystal Structure [22]	5
1.5 Phase Diagram for the Formation of SiC [24]	6
1.6 Phase Diagram for the Formation of SN Materials [34]	7
1.7 (a) α -Si ₃ N ₄ and (b) β - Si ₃ N ₄ Crystal Structure [35]	7
2.1 Effect of Naphthalene in Mechanical and Dielectric Properties of 35% SR-SN Ceramic Sintered at 1500 °C [87]	19
2.2 SEM Images of the LAS-SiC Nanocomposites [94]	22
2.3 SEM Images of the 50% Alumina-50% Mullite Ceramics: a) 1600 °C for 10 h; b) 1800 °C for 10 h [113]	28
2.4 (a) to (f) Stress-strain Curve for Compressive Strength of Porous Calcium Phosphate Ceramics for Biomedical Applications [120]	31
3.1 Preparation of sample (Mullite + SiC nanoparticles and Mullite + Si ₃ N ₄ nanoparticles)	33
3.2 Temperature Gradient for the Final Sintering Process	35
3.3 Principles of the Split Mould Configuration	38
3.4 Schematic Diagram of the 2 Point Dielectric Measurements Connected to Agilent 4294A Impedance Analyzer	41
3.5 Working Principle for Determining Thermal Diffusivity of a Material by the Laser Micro-flash Method [126]	42
3.6 Experimental Setup for Transmission Mode Measurement in the Laser Micro-flash System [127]	42
3.7 Compressive Stress/Strain Behavior (a) for ceramic samples; (b) 'Verdant' behavior [128]	44
4.1 Mullite Matrix Transitions Between 1000 °C to 1200 °C ('mk' denotes Metakaolin; 'M' for Mullite and γ -Al for γ -alumina. Errors for the XRD is defined at $\pm 0.5^\circ$)	46
4.2 XRD for SC-M Ceramic Pellets Sintered at 1000 °C. ('mk' denotes Metakaolin; 'M' for Mullite and 'SiC' for β -Silicon	48

	Carbide. Errors for the XRD is defined at $\pm 0.5^\circ$)	
4.3	XRD for SC-M Ceramic Pellets Sintered at 1100 °C. ('mk' denotes Metakaolin; 'M' for Mullite and 'SiC' for β -Silicon Carbide. Errors for the XRD is defined at $\pm 0.5^\circ$)	49
4.4	XRD for SC-M Ceramic Pellets Sintered at 1200 °C. ('mk' denotes Metakaolin; 'M' for Mullite, γ -Al for gamma alumina and 'SiC' for β -Silicon Carbide. Errors for the XRD is defined at $\pm 0.5^\circ$)	50
4.5	XRD for XRD for SN-M Ceramic Pellets Sintered at 1000 °C. ('mk' denotes Metakaolin and 'M' for Mullite. Errors for the XRD is defined at $\pm 0.5^\circ$)	51
4.6	XRD for SN-M Ceramic Pellet Sintered at 1100 °C. ('mk' denotes Metakaolin; 'M' for Mullite; ' α ' for α -Silicon Nitride and ' β ' for β -Silicon Nitride. Errors for the XRD is defined at $\pm 0.5^\circ$)	52
4.7	XRD for SN-M Ceramic Pellets Sintered at 1200 °C. ('mk' denotes Metakaolin; 'M' for Mullite; ' α ' for α -Silicon Nitride and ' β ' for β -Silicon Nitride. Errors for the XRD is defined at $\pm 0.5^\circ$)	53
4.8	Density Graph for the Mullite Matrix	54
4.9	Density of SC-M Ceramic Pellets Sintered at 1000 °C	55
4.10	Density of SC-M Ceramic Pellets Sintered at 1100 °C	56
4.11	Density of SC-M Ceramic Pellets Sintered at 1200 °C	57
4.12	Density Projection of the SC-M Ceramic Pellet from True and Bulk Density Estimations	58
4.13	Density of SN-M Ceramic Pellet Sintered at 1000 °C	59
4.14	Density of SN-M Ceramic Pellet Sintered at 1100 °C	60
4.15	Density of SN-M Ceramic Pellet Sintered at 1200 °C	61
4.16	Density Projection of the SN-M Ceramic Pellet from True and Bulk Density Estimations	62
4.17	Thermal Diffusivity of Mullite Matrix: a) in Normal Temperature x -axis and b) in $1/T$ Temperature x -axis	63
4.18	Thermal Diffusivity of SC-M Ceramic Pellet Sintered at 1000 °C: a) in Normal Temperature x -axis and b) in $1/T$ Temperature x -axis	64
4.19	Thermal Diffusivity of SC-M Ceramic Pellet Sintered at 1100 °C: a) in Normal Temperature x -axis and b) in $1/T$	66

	Temperature x -axis	
4.20	Thermal Diffusivity of SC-M Ceramic Pellet Sintered at 1200 °C: a) in Normal Temperature x -axis and b) in 1/T Temperature x -axis	67
4.21	Effect of SiC Concentration in Thermal Diffusivity of the 1000 °C SC-M Series Between 303 K to 773 K	68
4.22	Effect of SiC Concentration in Thermal Diffusivity of the 1100 °C SC-M Series Between 303 K to 773 K	68
4.23	Effect of SiC Concentration in Thermal Diffusivity of the 1200 °C SC-M Series Between 303 K to 773 K	69
4.24	Thermal Diffusivity for SN-M Ceramic Pellet Sintered at 1000 °C: a) in Normal Temperature x -axis and b) in 1/T Temperature x -axis	70
4.25	Thermal Diffusivity for SN-M Ceramic Pellet Sintered at 1100 °C: a) in Normal Temperature x -axis and b) in 1/T Temperature x -axis	71
4.26	Thermal Diffusivity for SN-M Ceramic Pellet Sintered at 1200 °C: a) in Normal Temperature x -axis and b) in 1/T Temperature x -axis	72
4.27	Effect of SN Concentration in Thermal Diffusivity of the 1000 °C SN-M Series Between 303 K to 773 K	73
4.28	Effect of SN Concentration in Thermal Diffusivity of the 1100 °C SN-M Series Between 303 K to 773 K	73
4.29	Effect of SN Concentration in Thermal Diffusivity of the 1200 °C SN-M Series Between 303 K to 773 K	74
4.30	Comparisons of the Sintering Temperature Effect on Thermal Diffusivity for SC-M Ceramic Pellets at 303K	75
4.31	Comparisons of the SiC Weight Additions Effect on Thermal Diffusivity for SC-M Ceramic Pellets at 303K	75
4.32	WEI Values for the SC-M Sintered at 1000 °C	76
4.33	WEI Values for the SC-M Sintered at 1100 °C	77
4.34	WEI Values for the SC-M Sintered at 1200 °C	77
4.35	Comparisons of the Sintering Temperature Effect on Thermal Diffusivity for SN-M Ceramic Pellets at 303 K	78
4.36	Comparisons of the SN Weight Addition Effect on Thermal Diffusivity for SN-M Ceramic Pellets at 303 K	79

4.37	WEI Values for the SN-M Sintered at 1000 °C	80
4.38	WEI Values for the SN-M Sintered at 1100 °C	80
4.39	WEI Values for the SN-M Sintered at 1200 °C	81
5.1 (a)-(e)	Compression Stress/Strain Graphs for the Mullite Matrix Cylinders for Samples (S1 – S5)	84
5.2	UCS Values for the Mullite Matrix Cylinders	87
5.3 (a)-(e)	Compression Stress/Strain Graphs for the 5% SC-M Cylinders for Samples (S1 – S5)	88
5.4	UCS Values for 5% SC-M Cylinders	90
5.5 (a)-(e)	Compression Stress/Strain Graphs for the 10% SC-M Cylinders for Samples (S1 – S5)	91
5.6	UCS Values for 10% SC-M Cylinders	93
5.7 (a)-(e)	Compression Stress/Strain Graphs for the 15% SC-M Cylinders for Samples (S1 – S5)	94
5.8	UCS Values for 15% SC-M Cylinders	96
5.9 (a)-(e)	Compression Stress/Strain Graphs for the 20% SC-M Cylinders for Samples (S1 – S5)	97
5.10	UCS Values for 20% SC-M Cylinders	99
5.11 (a)-(e)	Compression Stress/Strain Graphs for the 25% SC-M Cylinders for Samples (S1 – S5)	100
5.12	UCS Values for 25% SC-M Cylinders	102
5.13 (a)-(e)	Compression Stress/Strain Graphs for the 30% SC-M Cylinders for Samples (S1 – S5)	103
5.14	UCS Values for 30% SC-M Cylinders	105
5.15 (a)-(e)	Compression Stress/Strain Graphs for the 5% SN-M Cylinders for Samples (S1 – S5)	106
5.16	UCS Values for of 5% SN-M Cylinders	108
5.17 (a)-(e)	Compression Stress/Strain Graphs for the 10% SN-M Cylinders for Samples (S1 – S5)	109
5.18	UCS Values for 10% SN-M Cylinders	111
5.19 (a)-(e)	Compression Stress/Strain Graphs for the 15% SN-M Cylinders for Samples (S1 – S5)	112
5.20	UCS Values for 15% SN-M Cylinders	114

5.21	Compression Stress/Strain Graphs for the 20% SN-M Cylinders for Samples (S1 – S5)	115
5.22	UCS values for of 20% SN-M Cylinders	117
5.23	Compression Stress/Strain Graphs for the 25% SN-M Cylinders for Samples (S1 – S5)	118
5.24	UCS Values for 25% SN-M Cylinders	120
5.25	Compression Stress/Strain Graphs for the 30% SN-M Cylinders for Samples (S1 – S5)	121
5.26	UCS Values for 30% SN-M Cylinders	123
5.27	Density of the SC-M Cylinders, Before and After Sintering	124
5.28	WEI Values of the Density, Mass and Volume changes in SC-M	125
5.29	Comparisons of UCS over Density, Mass and Volume Ratios for SC-M Cylinders	126
5.30	Density of the SN-M Cylinders, Before and After Sintering	127
5.31	WEI Values of the Density, Mass and Volume changes in SN-M	127
5.32	Comparisons of UCS over Density, Mass and Volume Ratios for SN-M Cylinders	128
5.33	Comparison of the Upper, Average and Lower Limits of the Compressive Strength of the SC-M Composites in Terms of Weight Additions	129
5.34	Comparison of the Upper, Average and Lower Limits of the Compressive Strength of the SN-M Composites in Terms of Weight Additions	130
5.35	Comparison of the Compressive Strength Index to Weight Additions in Terms of Applied Pressure	131
5.36	Cross section of the Mullite Matrix Cylinder Fragments after Compression Test: (a) Compaction of Possible Voids, (b) Formation of Crack Fracture Line, (c) Magnification of the Fracture Line, and (d) Cross Section of a Mullite Matrix Control Sample	132
5.37	Cross section of the 5% SC-M Cylinder Fragments after Compression Test: (a) Cross Section of the Grain Separation, (b) Formation of Crack Fracture Line, (c) Magnification of the Fracture Line, and (d) Cross Section of 5% SC-M Control Sample	133
5.38	Cross section of the 10% SC-M Cylinder Fragments after Compression Test: (a) Cross Section of the Grain Separation, (b) Formation of Crack Fracture Line, (c) Magnification of the	134

	Fracture Line, and (d) Cross Section of 10% SC-M Control Sample	
5.39	Cross section of the 15% SC-M Cylinder Fragments after Compression Test: (a) Cross Section of the Grain Separation, (b) Formation of Crack Fracture Line, (c) Magnification of the Fracture Line, and (d) Cross Section of 15% SC-M Control Sample	135
5.40	Cross section of the 20% SC-M Cylinder Fragments after Compression Test: (a) Cross Section of the Grain Separation, (b) Formation of Crack Fracture Line, (c) Magnification of the Fracture Line, and (d) Cross Section of 20% SC-M Control Sample	136
5.41	Cross section of the 25% SC-M Cylinder Fragments after Compression Test: (a) Cross Section of the Grain Separation, (b) Formation of Crack Fracture Line, (c) Magnification of the Fracture Line, and (d) Cross Section of 25% SC-M Control Sample	138
5.42	Cross section of the 30% SC-M Cylinder Fragments after Compression Test: (a) Cross Section of the Grain Separation, (b) Formation of Crack Fracture Line, (c) Magnification of the Fracture Line, and (d) Cross Section of 30% SC-M Control Sample	139
5.43	Cross section of the 5% SN-M Cylinder Fragments after Compression Test: (a) Cross Section of the Grain Separation, (b) Formation of Crack Fracture Line, (c) Magnification of the Fracture Line, and (d) Cross Section of 5% SN-M Control Sample	140
5.44	Cross section of the 10% SN-M Cylinder Fragments after Compression Test: (a) Cross Section of the Grain Separation, (b) Formation of Crack Fracture Line, (c) Magnification of the Fracture Line, and (d) Cross Section of 10% SN-M Control Sample	141
5.45	Cross section of the 15% SN-M Cylinder Fragments after Compression Test: (a) Cross Section of the Grain Separation, (b) Formation of Crack Fracture Line, (c) Magnification of the Fracture Line, and (d) Cross Section of 15% SN-M Control Sample	142
5.46	Cross section of the 20% SN-M Cylinder Fragments after Compression Test: (a) Cross Section of the Grain Separation, (b) Formation of Crack Fracture Line, (c) Magnification of the Fracture Line, and (d) Cross Section of 20% SN-M Control Sample	143
5.47	Cross section of the 25% SN-M Cylinder Fragments after Compression Test: (a) Cross Section of the Grain Separation, (b)	144

	Formation of Crack Fracture Line, (c) Magnification of the Fracture Line, and (d) Cross Section of 25% SN-M Control Sample	
5.48	Cross section of the 30% SN-M Cylinder Fragments after Compression Test: (a) Cross Section of the Grain Separation, (b) Formation of Crack Fracture Line, (c) Magnification of the Fracture Line, and (d) Cross Section of 30% SN-M Control Sample	146
5.49	UCS of Composite to Mullite Ratio vs. Weight Addition of the Nanoparticles	148
6.1	Dielectric Behavior for Mullite Matrix Sintered at 1000 °C a) Dielectric Behavior at 30 °C; b) Relative Dielectric Permittivity From 100 °C to 400 °C	151
6.2	Dielectric Behavior for Mullite Matrix Sintered at 1100 °C a) Dielectric Behavior at 30 °C; b) Relative Dielectric Permittivity From 100 °C to 400 °C	153
6.3	Dielectric Behavior for Mullite Matrix Sintered at 1200 °C a) Dielectric Behavior at 30 °C; b) Relative Dielectric Permittivity From 100 °C to 400 °C	154
6.4	Dielectric Behavior for β -SiC Nanoparticles (moulded in similar Pellet Dimensions) a) Dielectric Behavior at 30 °C; b) Relative Dielectric Permittivity From 100 °C to 400 °C	155
6.5	Dielectric Behavior for SN Nanoparticles (moulded in similar Pellet Dimensions) a) Dielectric Behavior at 30 °C; b) Relative Dielectric Permittivity From 100 °C to 400 °C	157
6.6	Dielectric Behavior for 5% SC-M Sintered at 1000 °C a) Dielectric Behavior at 30 °C; b) Relative Dielectric Permittivity From 100 °C to 400 °C	158
6.7	Dielectric Behavior for 5% SC-M Sintered at 1100 °C a) Dielectric Behavior at 30 °C; b) Relative Dielectric Permittivity From 100 °C to 400 °C	159
6.8	Dielectric Behavior for 5% SC-M Sintered at 1200 °C a) Dielectric Behavior at 30 °C; b) Relative Dielectric Permittivity From 100 °C to 400 °C	160
6.9	Dielectric Behavior for 10% SC-M Sintered at 1000 °C a) Dielectric Behavior at 30 °C; b) Relative Dielectric Permittivity From 100 °C to 400 °C	162
6.10	Dielectric Behavior for 10% SC-M Sintered at 1100 °C a) Dielectric Behavior at 30 °C; b) Relative Dielectric Permittivity From 100 °C to 400 °C	163

6.11	Dielectric Behavior for 10% SC-M Sintered at 1200 °C a) Dielectric Behavior at 30 °C; b) Relative Dielectric Permittivity From 100 °C to 400 °C	164
6.12	Dielectric Behavior for 15% SC-M Sintered at 1000 °C a) Dielectric Behavior at 30 °C; b) Relative Dielectric Permittivity From 100 °C to 400 °C	165
6.13	Dielectric Behavior for 15% SC-M Sintered at 1100 °C a) Dielectric Behavior at 30 °C; b) Relative Dielectric Permittivity From 100 °C to 400 °C	166
6.14	Dielectric Behavior for 15% SC-M Sintered at 1200 °C a) Dielectric Behavior at 30 °C; b) Relative Dielectric Permittivity From 100 °C to 400 °C	167
6.15	Dielectric Behavior for 20% SC-M Sintered at 1000 °C a) Dielectric Behavior at 30 °C; b) Relative Dielectric Permittivity From 100 °C to 400 °C	168
6.16	Dielectric Behavior for 20% SC-M Sintered at 1100 °C a) Dielectric Behavior at 30 °C; b) Relative Dielectric Permittivity From 100 °C to 400 °C	169
6.17	Dielectric Behavior for 20% SC-M Sintered at 1200 °C a) Dielectric Behavior at 30 °C; b) Relative Dielectric Permittivity From 100 °C to 400 °C	170
6.18	Dielectric Behavior for 25% SC-M Sintered at 1000 °C a) Dielectric Behavior at 30 °C; b) Relative Dielectric Permittivity From 100 °C to 400 °C	171
6.19	Dielectric Behavior for 25% SC-M Sintered at 1100 °C a) Dielectric Behavior at 30 °C; b) Relative Dielectric Permittivity From 100 °C to 400 °C	172
6.20	Dielectric Behavior for 25% SC-M Sintered at 1200 °C a) Dielectric Behavior at 30 °C; b) Relative Dielectric Permittivity From 100 °C to 400 °C	173
6.21	Dielectric Behavior for 30% SC-M Sintered at 1000 °C a) Dielectric Behavior at 30 °C; b) Relative Dielectric Permittivity From 100 °C to 400 °C	174
6.22	Dielectric Behavior for 30% SC-M Sintered at 1100 °C a) Dielectric Behavior at 30 °C; b) Relative Dielectric Permittivity From 100 °C to 400 °C	175
6.23	Dielectric Behavior for 30% SC-M Sintered at 1200 °C a) Dielectric Behavior at 30 °C; b) Relative Dielectric Permittivity From 100 °C to 400 °C	176
6.24	Dielectric Behavior for 5% SN-M Sintered at 1000 °C a) Dielectric Behavior at 30 °C; b) Relative Dielectric Permittivity	178

From 100 °C to 400 °C

6.25	Dielectric Behavior for 5% SN-M Sintered at 1100 °C a) Dielectric Behavior at 30 °C; b) Relative Dielectric Permittivity From 100 °C to 400 °C	179
6.26	Dielectric Behavior for 5% SN-M Sintered at 1200 °C a) Dielectric Behavior at 30 °C; b) Relative Dielectric Permittivity From 100 °C to 400 °C	180
6.27	Dielectric Behavior for 10% SN-M Sintered at 1000 °C a) Dielectric Behavior at 30 °C; b) Relative Dielectric Permittivity From 100 °C to 400 °C	181
6.28	Dielectric Behavior for 10% SN-M Sintered at 1100 °C a) Dielectric Behavior at 30 °C; b) Relative Dielectric Permittivity From 100 °C to 400 °C	182
6.29	Dielectric Behavior for 10% SN-M Sintered at 1200 °C a) Dielectric Behavior at 30 °C; b) Relative Dielectric Permittivity From 100 °C to 400 °C	183
6.30	Dielectric Behavior for 15% SN-M Sintered at 1000 °C a) Dielectric Behavior at 30 °C; b) Relative Dielectric Permittivity From 100 °C to 400 °C	184
6.31	Dielectric Behavior for 15% SN-M Sintered at 1100 °C a) Dielectric Behavior at 30 °C; b) Relative Dielectric Permittivity From 100 °C to 400 °C	185
6.32	Dielectric Behavior for 15% SN-M Sintered at 1200 °C a) Dielectric Behavior at 30 °C; b) Relative Dielectric Permittivity From 100 °C to 400 °C	187
6.33	Dielectric Behavior for 20% SN-M Sintered at 1000 °C a) Dielectric Behavior at 30 °C; b) Relative Dielectric Permittivity From 100 °C to 400 °C	188
6.34	Dielectric Behavior for 20% SN-M Sintered at 1100 °C a) Dielectric Behavior at 30 °C; b) Relative Dielectric Permittivity From 100 °C to 400 °C	189
6.35	Dielectric Behavior for 20% SN-M Sintered at 1200 °C a) Dielectric Behavior at 30 °C; b) Relative Dielectric Permittivity From 100 °C to 400 °C	190
6.36	Dielectric Behavior for 25% SN-M Sintered at 1000 °C a) Dielectric Behavior at 30 °C; b) Relative Dielectric Permittivity From 100 °C to 400 °C	192
6.37	Dielectric Behavior for 25% SN-M Sintered at 1100 °C a) Dielectric Behavior at 30 °C; b) Relative Dielectric Permittivity From 100 °C to 400 °C	193

6.38	Dielectric Behavior for 25% SN-M Sintered at 1200 °C a) Dielectric Behavior at 30 °C; b) Relative Dielectric Permittivity From 100 °C to 400 °C	194
6.39	Dielectric Behavior for 30% SN-M Sintered at 1000 °C a) Dielectric Behavior at 30 °C; b) Relative Dielectric Permittivity From 100 °C to 400 °C	195
6.40	Dielectric Behavior for 30% SN-M Sintered at 1100 °C a) Dielectric Behavior at 30 °C; b) Relative Dielectric Permittivity From 100 °C to 400 °C	197
6.41	Dielectric Behavior for 30% SN-M Sintered at 1200 °C a) Dielectric Behavior at 30 °C; b) Relative Dielectric Permittivity From 100 °C to 400 °C	198
6.42	Dielectric Performance of the SC-M Pellets Sintered at 1000 °C (a) 1 KHz Response and (b) 1 MHz Response	199
6.43	Dielectric Performance of the SC-M Pellets Sintered at 1100 °C (a) 1 KHz Response and (b) 1 MHz Response	200
6.44	Dielectric Performance of the SC-M Pellets Sintered at 1200 °C (a) 1 KHz Response and (b) 1 MHz Response	201
6.45	Dielectric Performance of the SC-M Pellets (Sintered at 1000 °C) Against β -SiC Nanoparticle Weight Additions in: a). 1 KHz and b).1 MHz	202
6.46	Dielectric Performance of the SC-M Pellets (Sintered at 1100 °C) Against β -SiC Nanoparticle Weight Additions in: a).1 KHz and b). 1 MHz	204
6.47	Dielectric Performance of the SC-M Pellets (Sintered at 1200 °C) Against β -SiC Nanoparticle Weight Additions in: a). 1 KHz and b). 1 MHz.	205
6.48	Dielectric Performance of the SN-M Pellets Sintered at 1000 °C (a) 1 KHz Response and (b) 1 MHz Response	206
6.49	Dielectric Performance of the SN-M Pellets Sintered at 1100 °C (a) 1 KHz Response and (b) 1 MHz Response.	207
6.50	Dielectric Performance of the SN-M Pellets Sintered at 1200 °C (a) 1 KHz Response and (b) 1 MHz Response	208
6.51	Dielectric Performance of the SN-M Pellets (Sintered at 1000 °C) Against SN Nanoparticle Weight Additions in: a). 1 KHz and b). 1 MHz	209
6.52	Dielectric Performance of the SN-M Pellets (Sintered at 1100 °C) Against SN Nanoparticle Weight Additions in: a). 1 KHz and b). 1 MHz.	210

6.53	Dielectric Performance of the SN-M Pellets (Sintered at 1200 °C) Against SN Nanoparticle Weight Additions in: a). 1 KHz and b). 1 MHz	211
6.54	WEI Values of the SC-M Pellets to the Mullite Matrix With Respect To the Sintering Temperature Performance at 1 KHz	213
6.55	WEI Values of the SC-M Pellets to the Mullite Matrix With Respect To the Sintering Temperature Performance at 1 MHz	214
6.56	WEI Values of the SC-M Pellets to the Mullite Matrix With Respect To the Sintering Temperature Performance at 1 KHz	216
6.57	WEI Values of the SC-M Pellets to the Mullite Matrix With Respect To the Sintering Temperature Performance at 1 MHz	217

LIST OF ABBREVIATIONS

α	Thermal Diffusivity
α -SiC	alpha Silicon Carbide (hexagonal)
α -SN	alpha Silicon Nitride (trigonal)
ASTM	American Society for Testing and Materials
β -SiC	beta Silicon Carbide (cubic)
β -SN	beta Silicon Nitride (hexagonal)
C_H	Specific Heat Capacity of the material
C_P	Capacitance in Parallel Mode (Chapter 3)
ϵ_0	Permittivity at Vacuum
ϵ_r	Relative Dielectric Permittivity
ϵ_s	Static Dielectric Permittivity
ϵ_∞	Infinite Dielectric Permittivity
σ	Standard Deviation of UCS
f	Frequency
AC	Alternating Current
EDX	Energy Dispersive X-Rays
FESEM	Field Emission Scanning Electron Microscope
G	Conductance
HFH	High Frequency Hopping
λ	Thermal Conductivity
LFD	Low Frequency Dispersion
\ln/\ln	Exponential Logarithm
ρ	Density of material (gcm^{-3})
ρ_c	Density of a Composite Material
ρ_f	Density of the Filler Material
ρ_m	Density of the Matrix Material
\varnothing	Diameter

psi	Pounds per square inch
QDC	Quasi Direct current Conductivity
R	Resistance
rpm	Revolutions per Minute
SC-M	Silicon Carbide-Mullite Ceramic
SiC	Silicon Carbide
SN	Silicon Nitride
SN-M	Silicon Nitride-Mullite Ceramic
UCS	Ultimate Compressive Strength
UCS/m	Ultimate Compressive Strength to mass ratio
UCS/ ρ	Ultimate Compressive Strength to density ratio
UCS/v	Ultimate Compressive Strength to volume ratio
UTS	Universal Testing System
V	Voltage
$\langle \bar{v} \rangle$	Mean Average Electron Velocity
vol. %	Volume %
WEI	Work Efficiency Index
wt. %	Weight %
XRD	X-ray Diffraction

CHAPTER 1

INTRODUCTION

1.1 Introduction

When Prof. Richard P. Feynman gave the famous lecture entitled “There’s plenty of room at the bottom” [1], the emergence of nano-technology has begun in the ceramic material research. This paradigm has advanced beyond the conventional ceramic materials prevalent in current refractory ceramic industries. Since then, the research into material has delved into making smaller size materials and the characterizations of the resultant materials yielded surprisingly better properties compared to the micron sized ceramics [2].

In conventional refractory ceramics, there was no need to pursue the miniaturization of the material grain size as the industrial demands and cost of the raw material used do not allow it. Hence, the expansion of nanotechnology in this small field related to clays and aluminosilicates was restricted to novel research or thermal insulation panels where higher prices could be negotiated.

In the 1990s, thanks to Schneider et al. [3], the importance of pursuing research of mullite came back as the material provides good structural and functional electrical properties. Mullite has low thermal expansion, low electrical conductivity and high creep resistance, which provides good electrical and thermal insulation for high temperature electronics [4]. Since then, mullite based material have served as a potential high temperature gas filters [5] and heat exchangers [6].

However, the advancements of mullite in new applications have been restricted to process modification like mullite thin films [7], mullite coatings [8], mullite whiskers [9], or mullite fibers [10]. Therefore, the focus has been on reducing and reusing the mullite through size reduction of mullite. However, emphasis should be placed on exploiting the advantages of mullite in high temperature operations as matrix composite. The mullite matrix composites with platelet and particle fillers have been explored by Schneider and Okada [11]. The major focus has been directed at zirconium and silica as the main filler components [12] with application in mechanical and thermal properties.

As such, this research is directed towards the utilization of the Malaysian kaolinite as the starting precursor for the mullite matrix. The fillers used were silicon carbide (SiC) and silicon nitride (SN) nanopowders procured from the industry to ensure repeatable quality.

1.2 Research Background

Kaolinite has been a major constituent for ball clay/china clay for the making of porcelain and refractory materials [13]. It is used for fine china and commercial porcelain wares. Modern products that use kaolinite clay include glossy paper, toothpaste and geo-polymers fibers [14]. The consumption of kaolinite in United States of America by United States Geology Survey (USGS) is estimated at 5830 metric tons per year (refer to Figure 1.1) [14]. The current price per ton for kaolinite clay export is around USD 147-150 [14]. The Malaysian Geology department estimates the Malaysian kaolinite production at 35 metric tons per year [15]. Hence, kaolinite is a major ceramic raw material for modern productions.

	Bentonite		Mine production Fuller's earth		Kaolin	
	2013	2014 ^e	2013	2014 ^e	2013	2014 ^e
United States (sales)	4,350	4,660	² 1,990	² 2,070	5,950	5,830
Brazil (beneficiated)	513	500	—	—	2,200	1,800
Czech Republic (crude)	226	230	—	—	3,110	3,110
Germany (sales)	375	350	—	—	4,900	4,500
Greece (crude)	1,000	1,000	—	—	—	—
Italy	110	100	3	3	640	640
Mexico	618	620	108	100	163	160
Spain	115	100	593	590	303	250
Turkey	1,100	1,100	—	—	3,800	3,800
Ukraine (crude)	210	180	—	—	1,100	1,100
United Kingdom (sales)	—	—	—	—	900	900
Uzbekistan (crude)	25	25	—	—	7,500	7,000
Other countries	3,360	3,300	306	270	9,730	11,000
World total (rounded)	12,000	12,200	² 3,000	² 3,000	40,300	41,000

Figure 1.1: Global Consumption of Kaolin Clay [14].

However, there is a major shortcoming with kaolinite material. As kaolinite is mined geographically by each country, the kaolinite material differs in alumina-silica concentration and impurities depending on the mining source. Hence, kaolinite material from Georgia, USA will differ from Indian kaolinite and Malaysian kaolinite both in material composition and resulting products.

1.3 Problem Statement

Despite kaolinite being one of Malaysia's clay exports (with majority of them produced from Bidor-Tapah area), the production of Malaysian kaolinite has decreased by 10% in 2013 compared to 2012 values at 442.5 metric tons [15]. The slow decline in kaolinite production may be related to the market forces, but the Malaysian kaolinite is currently exported as a raw material with little processing rather as a finished product. Hence, a paradigm shift is necessary in adding value to the Malaysian kaolinite products industry.

The current advances in pushing materials towards nano-size levels and mono-layered materials like graphene, has pushed them towards composite formation of micron matrix with nanoparticle fillers, which are rare in the material literature. So far, the literature in this aspect has been on by SiC-mullite composition with

emphasis on thermal and mechanical applications (refer to section 2.5 and 2.6 of Chapter 2).

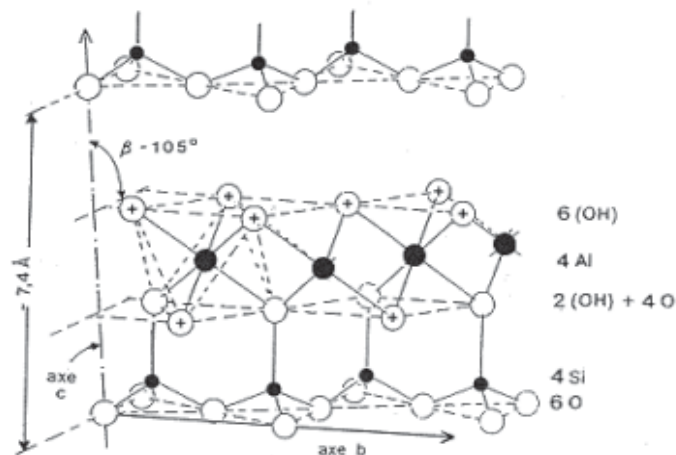
This research hopes to replicate part of the SiC-mullite with industry based standard materials obtained from kaolinite and SiC nanopowders. The insertion of foreign particles into mullite materials (sintered from kaolinite at 1000 °C to 1200 °C) is not well researched as the particle distributions and mullite growth mechanism (in response to particles) in this region affects the final composition morphology obtained by acicular mullite at 1500 °C to 1700 °C.

The research will also explore the application of inserting SN nanoparticles in the mullite matrix phase with similar methodology. This composition mix has not been tested in the research literature, especially in the nanopowder region. This pilot project will characterize the electrical, thermal and mechanical (uniaxial compression) properties for the SiC-mullite and SN-mullite composites.

1.4 Matrix Information

Kaolinite is a common aluminosilicate clay material formed from the weathering process of basalt rocks. It was named after the word ‘kaoling’ in China [16]. It is a main ingredient in the process of making fine china or bone china ceramics. According to USGS Clay summary report [14], the usage of kaolinite material in US domestic market is mainly in paper manufacturing. Other uses of kaolinite raw powder include: filler and extender for paint, plastic and rubber products.

The kaolinite structure is unique in nature as the water molecules are sandwiched between the alumina and silica layers [17]. The sandwich water layer is a result of the natural rock weathering process due to slow absorption of the water molecule into the rock and/or minerals through centuries. So far, this process could not be replicated synthetically. However, the sandwich water removal during the sintering will deconstruct the aluminosilicate structure [17]. Figure 1.2 compares the same monolayer of the alumina-silica composition as a result of the water removal [18].



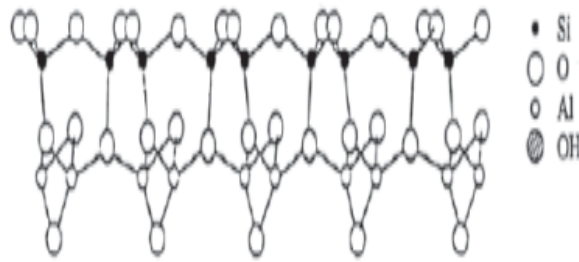


Figure 1.2: Kaolinite and Mullite Crystal Structure [18].

The sintering of kaolinite will produce different aluminosilicate products depending on the soaking temperature used. Details of the aluminosilicate process are explained in section 4.2 of Chapter 4, with the XRD data of the pure kaolinite-mullite matrix. The products of the kaolinite conversion are metakaolin, γ -alumina (also known as spinel aluminum-silica) and mullite. Each product depends on the reaction temperature of the kaolinite-mullite transformation (Figure 1.3).

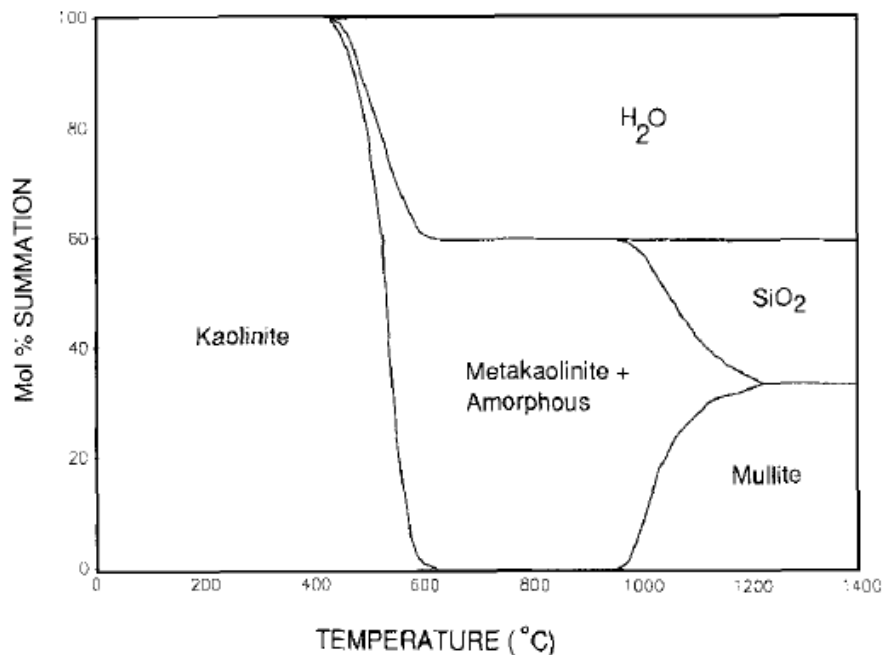


Figure 1.3: Phase Diagram for the Kaolinite to Mullite Transformation [19]

1.5 Filler Information

1.5.1 Silicon Carbide (SiC)

Silicon carbide (SiC) is a synthetic product produced from silicon and carbon. There are natural deposits of SiC called Moissanite, which are rare and found mostly in crater sites resulting from meteorites crash sites. The bonding of silicon and carbon requires intense heat and pressure to create covalent bonding between the silicon and carbon atoms [20].

SiC materials usually result in polytypes as variations of the Si-C-Si-C stacking order in layers [21]. There are three common polytypes stacking orders: namely 3c-SiC (also known as β -SiC), 4h-SiC and 6h-SiC (known as α -SiC), which are illustrated in Figure 1.4. The differences between them are the resultant crystal form and the number of repeating stacking order: c and h denotes cubic and hexagonal crystal form whereas the 3, 4 and 6 denote the layers per stacking sequence.

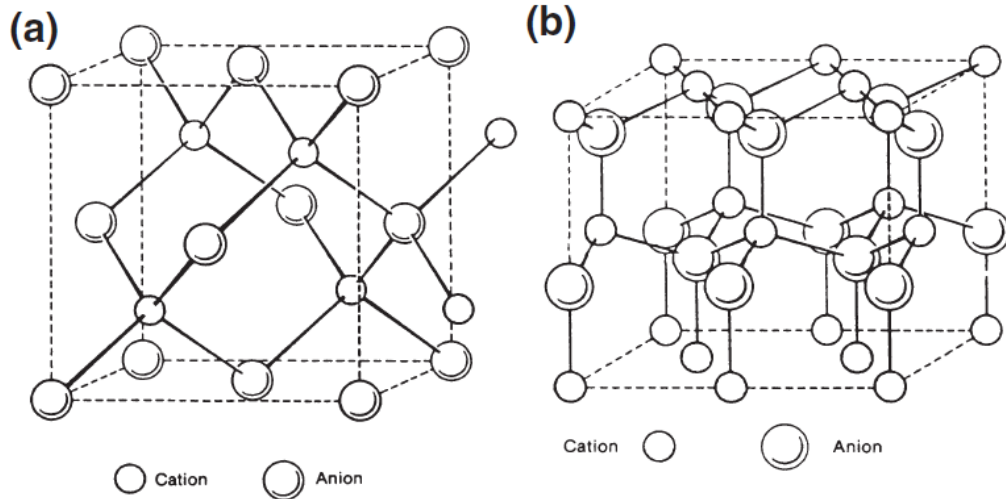


Figure 1.4: (a) β -SiC and (b) α -SiC Crystal Structure [22].

Both α and β polytypes are the most commonly produced SiC crystals. The α -SiC are formed above 1700 °C. Temperatures below the 1700 °C temperature mark usually result in the β -SiC formation [23]. The SiC does not melt at high temperature of 2700 °C; instead it decomposes into Si (liquid) and C (gas). This process is also known as sublimation. This makes SiC a useful material for high temperature applications.

Synthetic pure SiC crystals are colorless and transparent, whereas the industrial products can vary from black, grey to green in color depending on the impurities present. The production of SiC results from the pressurized, vacuum sintering of silicon and carbon. The presence or vacuum or pressurized inert gases are needed because the carbon has higher affinity to oxygen compared to the silicon. Therefore, there is a possibility of minute silica (SiO_2) crystals in between the SiC crystals.

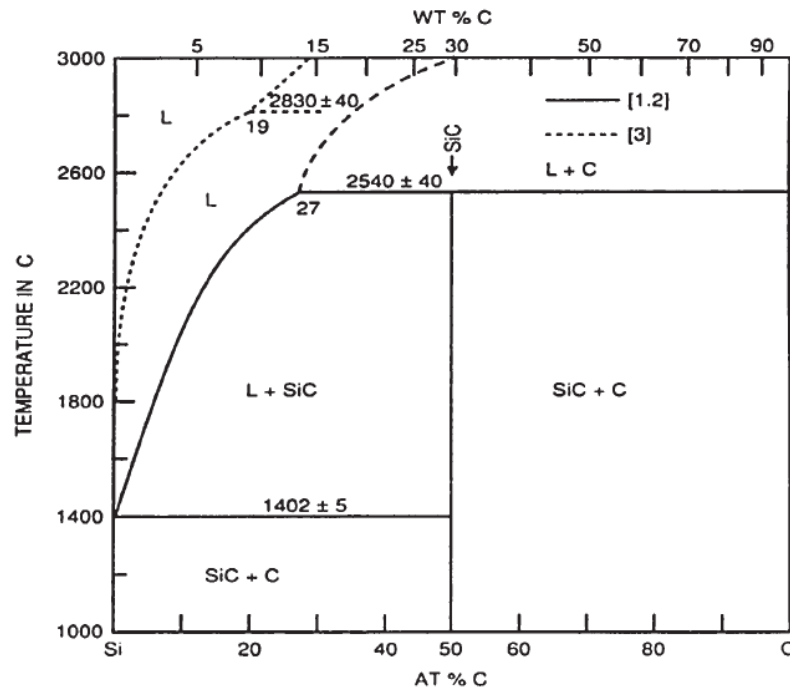


Figure 1.5: Phase Diagram for the Formation of SiC [24]

Conventional process include the Acheson and Lely methods of producing micron size SiC crystals [25]. Referring to Figure 1.5, the temperatures needed to sustain Acheson reaction is above 1800 °C for 30 atomic % to 40 atomic % of carbon present. Hence, modern nano-materials processing technology developed lower temperature reactions such as plasma enhanced chemical vapor deposition (PECVD) to mass produce SiC nanopowders in large quantities with controlled grain sizes and polytypes orders [26].

Applications of the SiC include modern abrasives and cutting tools for metalwork; electronic components such as MOSFETS and transistors [27], diodes and LEDs [28]. It is also used for mirrors for radiation sensors [29], nuclear fuel particles and cladding systems [30]. Current research also focuses on its ability as a catalyst and possible graphene starter material [31].

1.5.2 Silicon Nitride (SN)

Silicon nitride (SN) consists of three Silicon atoms bonded covalently to 4 Nitrogen atoms. It is a man made compounds as the natural mineral sources of SN compounds are not found underground except for Nierite mineral, which is found in meteorite craters [32]. The phase diagram for the synthesis of SN is shown in Figure 1.6.

Common SN materials have three different crystal structures, namely, trigonal, hexagonal and cubic structure. Both trigonal and hexagonal SN structures are known as α - and β -SN. Both materials displayed stacking layers as ABCD-ABCD layers (in α -SN) AB-AB layers (in β) [33]; both structures are shown in Figure 1.7. The last

structure is known γ -SN, which has a spinel cubic crystal structure similar to boron nitride [33]. Of the three crystal structures, β -SN is the most stable and major form of SN in ceramic production.

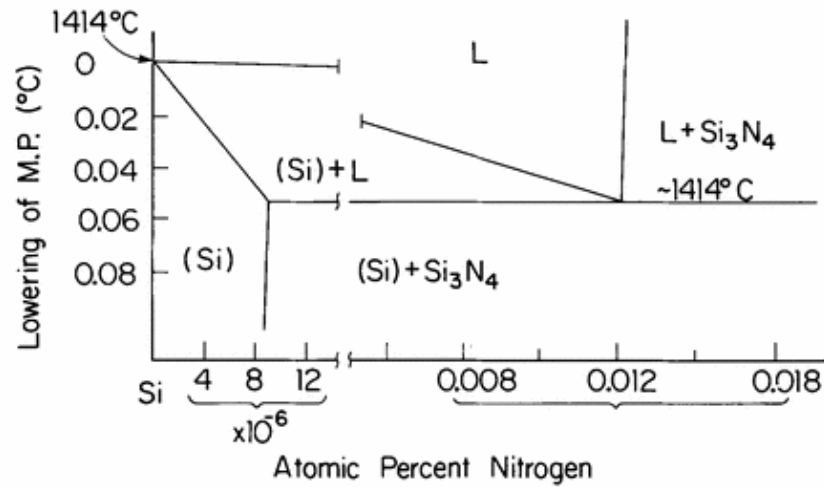


Figure 1.6: Phase Diagram for the Formation of SN Materials [34]

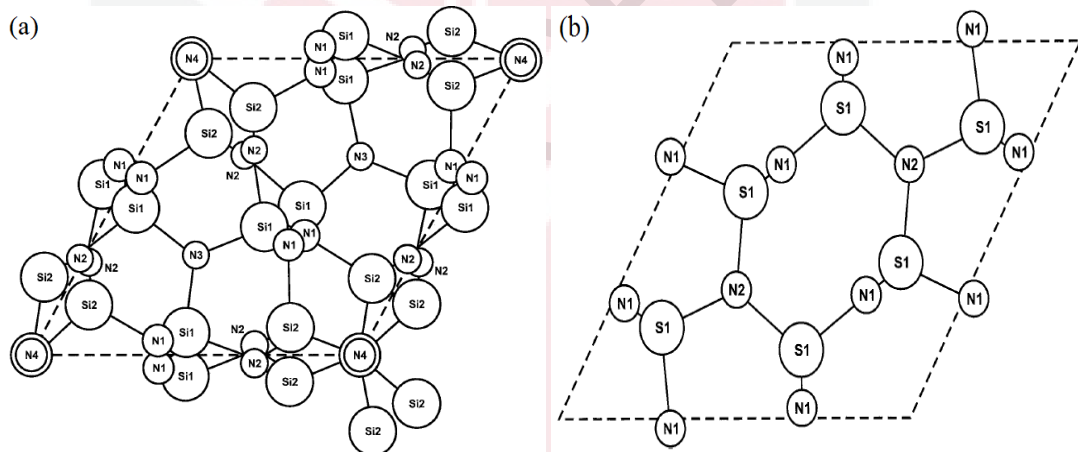


Figure 1.7: (a) α -SN and (b) β -SN Crystal Structure [35]

Applications of the SN ceramics materials are wear resistance materials such as bearings and engine components [36]; high temperature material such as rocket thrusters [37]; cuttings tools [38]; electronics (but not as a semiconductor like SiC, but as insulating masks) [39].

1.6 Theoretical Framework

SiC and SN nano-materials have been well researched as composite materials for applications into thermal, mechanical and electrical improvements [40 - 44]. The reduction in grain sizes compared to their micron counterparts has increased the electrical and mechanical properties of the materials as the miniaturization allows for

larger surface to volume ratio. This in turn affects the electronic transport and chemical bonding properties significantly and enhances the overall material.

However, the fore-mentioned literature examines the single phase aspect of the nano-material enhancement. The improvement in electrical thermal and mechanical properties proven by the nanomaterials should function well as an intermediate material between the micron size materials. Therefore, the mullite derived from the industry sector would be elevated by the addition of the nanoparticles during the sintering. The selection of mullite, SiC and SN are carefully considered in both chemical reactivity and thermal expansion in relation to each other during the sintering environment. Following the theory of concrete application, the smaller sizes of the nanomaterials will fill in the voids of the micron grain gaps and provide higher mechanical strength in uniaxial compression tests.

Similarly, thermal diffusivity of the composite material will increase due to the fused contact between the nanomaterials and micron materials. The heat transfer across the material will be easier as the radiation propagation is bypassed and the heat is transferred via the phonon and vibration across the medium. For steady state systems, thermal conductivity (α) represents the temperature gradient changes governed by Fourier's Law (refer to equation 1.1) [45]. For composites materials with random filler orientation, the temperature gradient becomes a transient state system, which dependent on variations in heat capacity and density at different temperatures [45].

$$\frac{dT}{dt} = a \cdot \nabla^2 T \quad (1.1)$$

Where dT/dt represents the temperature gradient across the material, a is the thermal conductivity (steady state systems); thermal diffusivity (transient systems) and T is the measuring temperature.

In this research, SiC and SN nanoparticles functions as porosity control within the mullite structure, which dictates a possible lower and transient temperature gradient based on the random distribution of the nanoparticles. The composite system would also contain trapped air, which will reduce the overall thermal diffusivity of the composite system [45].

1.7 Conceptual Framework

The determination of the nanomaterials' enhancement will be tested against the properties of the original matrix itself. The index for the comparison will form the basis of whether the properties could be enhanced through physical means. A comparison index is defined as

$$P_{index} = \frac{P_{After Addition} - P_{Before Addition}}{P_{Before Addition}} \times 100\% \quad (1.2)$$

Where P can be defined as the tested property such as thermal diffusivity, Compression strength and relative dielectric permittivity. The resultant values would be in positive or negative numerical values. A positive would indicate enhancement; the negative value would show a suppressive element by the nanoparticles in the micron matrix material.

Of course, in order to safeguard the consistency of the experiments, both the matrix material and subsequent nanoparticle added composites would have to be processed and sintered according to the same methodology, which includes the delicate settings of the argon assisted sintering process. The testing protocol will be conducted in a similar fashion.

The research material in this project was selected from industry sources to ensure repeatability for the property testing. The research discourages its own production of the nanoparticles under testing to discourage any possible ‘black swan’ enhancement argument. All materials are bought from reputable manufacturers with specific production batches for quality and quantity control in cases of repeatability argument.

1.8 Research Objectives

Based on the problem statements section, this research project is focused on the following main research objectives:

1. To obtain a homogenous ceramic mix of the micron matrix and nanopowder in specific mix ratios will be produced.
2. To study both SC-M and SN-M series for structural, thermal (thermal diffusivity), mechanical (uniaxial compression) and electrical (low frequency dielectrics) properties.
3. To study and assess the level of enhancement between the properties of the mullite matrix against nanopowder filler in the mullite matrix in the characterization data collected in the second objective.

1.9 Research Limitations

In this research project, there are some limitations to the scope of research carried out in the investigation of the SC-M and SN-M ceramic composites. Some of the limitations are listed below:

1. The research matrix material is restricted to Malaysian sourced kaolinite as the purpose is to determine the properties in the kaolinite as starting matrix material for nanopowder enhancement.
2. The nanopowders used in this research are procured from an established nanopowder manufacturer (US Research Nanopowders, Inc.). This is to

ensure that there are no discrepancies or random deviations of the nano-materials.

3. Certain aspects of material process technology have to be designed specifically as there is no resource for the material fabrications. Hence, there are possible errors related to the design specification and safety use.
4. The process technologies of the composite are controlled to prevent the nanoparticles from oxidation attack. Therefore, the sintering process is restricted to the available controlled environment furnaces, which have a maximum operating temperature of 1200 °C in argon gas. This forms the upper limit for the sintering process in this research.
5. Not all data types of the characterization test are explored in this research. High frequency dielectric measurements, different operating temperatures, tensile and bending tests will be explored in the future work.



REFERENCES

- [1] Feynman, R. P. The Pleasure of Finding Things Out: The Best Short Works of Richard P. Feynman; Basic Books: New York, 1999; pp 117 - 140.
- [2] Colombo, P.; Mera, G.; Riedel, R.; Soraru, G. D. Polymer-Derived Ceramics: 40 Years of Research and Innovation in Advanced Ceramics”, *J. Am. Ceram. Soc.*, 2010 93[7], 1805 – 1837.
- [3] Schneider, H.; Voll, D.; Saruhan, B.; Sanz, J.; Schrader, G.; Ruscher, C.; Mosset, A. Synthesis and Structural Characterization of Non-Crystalline Mullite Precursors, *J. Non-Cryst. Solids*, 1994, 178, 262 – 271.
- [4] Okada, K.; Schneider, H. Chapter 4: Mullite Synthetic and Processing - Applications of Mullite Ceramics. In *Mullite*; Schneider, H.; Komarneni, S., Eds.; Wiley-VCH Verlag GmbH: Weinheim, Germany, 2005; pp 327 - 337.
- [5] Kitaoka, S.; Kawashima, N.; Komatsubara, Y.; Yamaguchi, A.; Suzuki, H. Improved Filtration Performance of Continuous Alumina-Fiber-Reinforced Mullite Composites for Hot-Gas-Cleaning, *J. Am. Ceram. Soc.*, 2005, Vol. 88[1], 45 – 50.
- [6] Girolamo, G. D.; Blasi, C.; Pilloni, L.; Schioppa, M. Microstructure and Thermal Properties of Plasma Sprayed Mullite Coatings, *Ceram. Int.*, 2010, 36, 1389 -1395.
- [7] Chen, Y. Y.; Wei, W. C. J. Formation of Mullite Thin Film via A Sol-Gel Process with Polyvinyl-pyrrolidone Additive, *J. Eur. Ceram. Soc.*, 2001, 21, 2435 –2540.
- [8] Hou, P.; Basu, S. N.; Sarin, V. K. Structure and High Temperature Stability of Compositionally Graded CVD Mullite Coatings, *Int. J. of Refract. Met. and Hard Mater.*, 2001, 19 [4-6], 467 - 477.
- [9] Choi, H. J.; Lee, J. G. Synthesis of Mullite Whiskers, *J. Am. Ceram. Soc.*, 2002, 85[2], 481 - 483.
- [10] Li, K.; Shimizu, T.; Igarashi, K. Preparation of Short Mullite Fibers from Kaolin via Addition of Foaming Agents, *J. Am. Ceram. Soc.*, 2001, 84[3], 497 - 503.
- [11] Okada, K.; Schneider, H. Chapter 7: Mullite Matrix Composites - Platelet and Particle Reinforced Mullite Matrix Composites. In *Mullite*; Schneider, H.; Komarneni, S., Eds.; Wiley-VCH Verlag GmbH: Weinheim, Germany, 2005; pp 443 - 463.
- [12] Descamps, P.; Sakaguchi, S.; Poorterman M.; Cambier, F. High Temperature Characterization of Reaction Sintered Mullite-Zirconia Composites, *J. Am. Ceram. Soc.* 1991, 74[10], 2476 - 2481.
- [13] Grimshaw, R. W. *The Chemistry and Physics of Clays and Other Allied Ceramic Materials*, 4th Ed.; Ernest Benn Limited: London, UK, 1971; pp 292 – 296.
- [14] Virta, R. L. *Materials Commodity Summaries 2015 – Clays*; Material Commodity Summary Series; U.S. Geological Survey, 2015; pp 18.1 - 18.20.
- [15] Tse, P. K. The Mineral Industry of Malaysia. In *USGS 2012 Minerals Yearbook – Malaysia [Advance Release]*; U.S. Geological Survey, 2013; pp 16.1 – 16.7.

- [16] Klein, C.; Dutrow, B. Chapter 19: Systemic Descriptions of Rock Forming Silicates- Clay Mineral Group –Kaolinite. In *The 23rd Edition of The Manual of Mineral Science*, 23rd Ed.; John Wiley and Sons Inc.: New Jersey, 2008; pp 522 – 523.
- [17] Sacks, M. D.; Pask, J. A. Sintering of Mullite-Containing Materials: I, Effect of Composition, *J. Am. Ceram. Soc.*, 1982, 65[2], 65 – 70.
- [18] Varga, G. The Structure of Kaolinite and Metakaolinite, *Epitoanyag*, [Online] 2007, 59, 6 – 9.
<http://en.epitoanyag.org.hu/static/upload/10.14382epitoanyag-jsbcm.2007.2.pdf> (Accessed 1st May 2015).
- [19] Pask, J. A.; Tomsia, A. P. Formation of Mullite from Sol-gel Mixtures and Kaolinite, *J. Am. Ceram. Soc.*, 1991, 74[10], 2367 - 2373.
- [20] Wu, R.; Zhou, K.; Yue, C. Y.; Wei, J.; Pan, Y. Recent Progress in Synthesis, Properties and Potential Applications of SiC Nanomaterials, *Prog. Mater. Sci.*, 2015, 72, 1 - 60.
- [21] Camassel, J.; Contreras, S.; Robert, J. L. SiC Materials: A Semiconductor Family for the Next Century, *Cr. Acad. Sci. IV*, 2000, 1[1], 5 - 21.
- [22] Kingery, W. D.; Bowen, H. K.; Uhlmann, D.R. *Introduction to Ceramics*, 2nd Ed.; John Wiley and Sons: New York, 1976; pp 63.
- [23] Olesinski, R. W.; Abbaschian, G. J. The C-Si (Carbon-Silicon) System, *Bull. Alloy Phase Diag.*, 1984, 5, 486 – 489.
- [24] Raygan, S.; Kondori, B.; Yangijeh, H. M. Effect of Mechanical Activation on the Production of SiC from Silica Sand, *Int. J. Refract. Met. Hard Mater.*, 2011, 29, 10 – 13.
- [25] Ulrich, S.; Theel, T.; Schwan, J.; Batori, V.; Schreib, M.; Ehrhardt, H. Low Temperature Formation of β - Silicon Carbide, *Diamond Relat. Mater.*, 1997, 6, 645 - 648.
- [26] Ouennoughi, Z.; Toumi, S.; Weiss, R. Study of Barrier Inhomogeneities Using I-V-T Characteristics of Mo/4H-SiC Schottky Diode, *Physica B*, 2015, 456, 176 – 181.
- [27] Suzuki, A.; Fujii, Y.; Saito, H.; Tajima, Y.; Furukawa, K.; Nakajima, S. Effect of the Junction Interface Properties on Blue Emission of Blue SiC LEDs Grown by Step Controlled CVD, *J. Cryst. Growth*, 1991, 115, 623 – 627.
- [28] Ha, J. H.; Kang, S. M.; Park, S. H.; Kim, H. S.; Lee, N. H.; Song, T. Y. A Self-Biased Neutron Detector Based on a SiC Semiconductor for Harsh Environment, *Appl. Radiat. Isot.*, 2009, 67, 1204 – 1207.
- [29] Kim, D.; Lee, H. G.; Park, J. Y.; Kim, W. J. Fabrication and Measurement of Hoop Strength of SiC Triplex Tube for Nuclear Cladding Applications, *J. Nucl. Mater.*, 2015, 458, 29 – 36.
- [30] Kim, J. G.; Kim, Y. H.; Lim, C. H.; Choi, D. J. Formation of Graphene on SiC by Chemical Vapor Deposition with Liquid Sources, *Surf. Coat. Technol.*, 2013, 231, 189 – 192.
- [31] Lee, M. R.; Russell, S. S.; Arden, J. W.; Pilinger, C. T. Nierite (Si_3N_4), A New Mineral from Ordinary and Enstatite Chondrites, *Meteorit. Planet. Sci.*, 1995, 30[4], 387 - 398.
- [32] Hong, P. *Spark Plasma Sintering of Si_3N_4 -Based Ceramics: Sintering Mechanism- Tailoring Microstructure-Evaluating Properties*. PhD. Thesis, Stockholm University, Stockholm, Sweden, 2004.

- [33] Wild, S.; Grieveson, P.; Jack, K. H. The Crystal Structures of Alpha and Beta Silicon and Germanium Nitrides. In *Special Ceramics: Vol. 5*; Popper, P., Ed.; British Ceramic Research Association: Stoke-on-Trent, U.K., 1972; pp 385 - 395.
- [34] Carlson, O. N. The N-Si (Nitrogen-Silicon) System, *Bull. Alloy Phase Diag.*, 1990, 11[6], 569.
- [35] Lin, H. T.; Ferber, M. K.; Becher, P. F.; Price, J. R.; van Roode, M.; Kimmel, J. B.; Jimenez, O. D. Characterization of First-Stage Silicon Nitride Components After Exposure to an Industrial Gas Turbine, *J. Am. Ceram. Soc.*, 2008, 89[1], 192 – 197.
- [36] Lange, F. F. Fracture Toughness of Si₃N₄ as Function of Initial α -Phase Content, *J. Am. Ceram. Soc.*, 1979, 62[7-8], 428G.
- [37] Riley, F. L. Silicon Nitride and Related Materials, *J. Am. Ceram. Soc.*, 2000, 83[2], 245 – 265.
- [38] Gwo, S. Scanning Probe Oxidation of Si₃N₄ Masks for Nanoscale Lithography, Micromachining and Selective Epitaxial Growth on Silicon, *J. Phys. Chem. Solids*, 2001, 62, 1673 – 1687.
- [39] Rahman, A.; Singh, A.; Harimkar, S. P.; Singh, R. P. Mechanical Characterization of Fine Grained Silicon Carbide Consolidated Using Polymer Pyrolysis and Spark Plasma Sintering, *Ceram. Int.*, 2014, 40, 12081 - 12091.
- [40] Li, Y.; Guo, Y.; Song, Q.; Li, H.; Fu, Q.; Li, K. Oxidation Pre-treatment and Electrophoretic Deposition of SiC Nanowires to Improve Thermal Shock Resistance Of SiC Coating for C/C Composites, *J. Alloys. Compd.*, 2015, 636, 165 – 170.
- [41] Parchoviansky, M.; Galusek, D.; Svancarek, P.; Sedlacek, J.; Sajgalik, P. Thermal Behavior, Electrical Conductivity and Microstructure of Hot Pressed Al₂O₃/SiC Nanocomposites, *Ceram. Int.*, 2014, 40, 14421 – 14429.
- [42] Derradji, M.; Ramdani, M.; Zhang, T.; Wang, J.; Lin, Z.; Yang, M.; Xu, X.; Liu, W. High Thermal and Thermomechanical Properties Obtained by Reinforcing a Bisphenol-A Based Phthalonitrile resin with Silicon Nitride Nanoparticles, *Mater. Lett.*, 2015, 149, 81 - 84.
- [43] Gonzalez-Julian, J.; Iglesias, Y.; Caballero, A. C.; Belmonte, M.; Garzon, L.; Ocal, C.; Miranzo, P. Multi-Scale Electrical Response of Silicon Nitride/Multi-walled Carbon Nanotubes Composites, *Compos.. Sci. Tech.*, 2011, 71, 60 – 66.
- [44] Blaß, U. W.; Barsukova, T. ; Schwarz, M. R.; Kohler, A.; Schimpf, C.; Petrusha, I. A.; Muhle, U.; Rafaja, D.; Kroke, E. Titanium Nitride Ceramics – Significant Enhancement of Hardness by Silicon Nitride Addition, Nanostructuring and High Pressure Sintering, *J. Eur. Ceram. Soc.*, 2015, 35, 2733 – 2744.
- [45] Figura, L. O.; A. A. Teixeira, *Food Physics Physical Properties – Measurement and Applications*; Springer Verlag: Berlin Heidelberg, 2007; pp 257 – 332.
- [46] Sivakumar, R.; Jeyaseelan, D. D.; Nishikawa, T.; Honda, S; Awaji, H. Influence of MgO on Microstructure and Properties of Mullite-Mo Composite Fabrication by Pulse Electrical Current Sintering, *Ceram Int.*, 2001, 27, 537 - 541.

- [47] Hayashi, K.; Kyaw, T. M.; Okamoto, Y. Thermal Properties of Mullite/Partially Stabilized Zirconia Composites, *High Temp. High Press.*, 1989, 30, 283 - 290.
- [48] Russell, L. M.; Donaldson, K.Y.; Hasselman, D. P. H.; Ruh, R.; Adams, J. W. Thermal Diffusivity/Conductivity and Specific Heat of Mullite-Zirconia-Silicon Carbide Whisker Composites, *J. Am. Ceram. Soc.*, 1996, 79, 2767 - 2770.
- [49] Hildmann, B.; Schneider, H. Thermal Conductivity of 2/1-Mullite Single Crystals, *J. Am. Ceram. Soc.*, 2005, 88[10], 2879 - 2882.
- [50] Schneider, H.; Eberhard, E. Thermal Expansion of Mullite, *J. Am. Ceram. Soc.*, 1990, 73[7], 2073 - 2076.
- [51] Guse, W.; Mateika, D. Growth of Mullite Single Crystals ($2\text{Al}_2\text{O}_3\cdot\text{SiO}_2$) by the Czochralski method, *J. Cryst. Growth*, 1974, 22, 237 - 240.
- [52] Chaudhuri, S. P.; Patra, S. K.; Chandraborty, A.K. Electrical Resistivity of Transition Metal Ion Doped Mullite, *J. Eur. Ceram. Soc.*, 1999, 19, 2941 - 2950.
- [53] Malki, M.; Hoo, C.H.; Mecartney, M. L.; Schneider, H. Electrical Conductivity of Mullite Ceramics, *J. Am. Ceram. Soc.*, 2014, 97[6], 1923 - 1930.
- [54] Ruh, R.; Chievezer, H. M. Permittivity and Permeability of Mullite-SiC Whisker and Spinel-SiC Whisker Composites, *J. Am. Ceram. Soc.*, 1998, 81[4], 1069 - 1070.
- [55] Somiya, S.; Hirata, Y. Mullite Powder Technology and Applications in Japan, *Am. Ceram. Soc. Bull.*, 1991, 70, 1624 - 1632.
- [56] Kanzaki, S.; Tabata, H.; Kumazawa, T.; Ohta, S. Sintering and Mechanical Properties of Stoichiometric Mullite, *J. Am. Ceram. Soc.*, 1985, 68[1], C6 - C7.
- [57] Ismail, M. G. M. U.; Nakai, Z.; Minegishi, S.; Somiya, S. Microstructure and Mechanical Properties of Mullite Prepared by the Sol-gel Method, *J. Am. Ceram. Soc.*, 1987, 70[1], C7 - C8.
- [58] Ohira, H.; Ismail, M. G. M. U.; Yamamoto, Y.; Akiba, T.; Somiya, S. Mechanical Properties of High Purity Mullite at Elevated Temperatures, *J. Eur. Ceram. Soc.*, 1996, 16, 225 - 229.
- [59] Kumazawa, T.; Kanzaki, S.; Ohta, S.; Tabata, H. Influence of Chemical Composition on the Mechanical Properties of $\text{SiO}_2\text{-Al}_2\text{O}_3$ Ceramics, *J. Ceram. Soc. Jpn.*, 1988, 65, 85 - 91.
- [60] Itoh, M.; Hamano K.; Okada, S. Preparation of Mullite Ceramics from Kaolin and Aluminum Hydroxide. In *Abstracts of the Third Symposium on Ceramics - Paper no 6-2A13*, Ceramics Society of Japan: Tokyo, Japan, 1990; pp 2A13.
- [61] Mizuno, M.; Sato, H. Preparation of Highly Pure Fine Mullite Powder, *J. Am. Ceram. Soc.*, 1989, 72[3], 377 - 382.
- [62] Scace, R. I.; Slack, G. A. Solubility of Carbon in Silicon and Germanium, *J. Chem. Phys.*, 1959, 30, 1551 - 1555.
- [63] Burgemeister, E. A.; von Muench, W.; Pettenpaul, E. Thermal Conductivity and Electrical Properties of 6H Silicon Carbide, *J. Appl. Phys.*, 1979, 50[9], 5790 - 5794.

- [64] Morelli, D.; Hermans, C. Beetz, C.; Woo, W. S.; Harris, G. L.; Taylor, C. *Silicon Carbide and Related Materials*. Spencer, M. G.; Devaty, R.P.; Edmond, J. A.; Khan, M. A.; Kaplan, R.; Rahaman, M. N., Eds., Institute of Physics Conference Series, N137, 1993, pp 313 - 316.
- [65] Volz, E.; Roosen, A.; Hartung W.; Winnaker, A. Electrical and Thermal Conductivity of Liquid Phase Sintered SiC, *J. Eur. Ceram. Soc.*, 2001, 21, 2089 – 2093.
- [66] Nilsson, O.; Mehling, H.; Horn, R.; Fricke, J.; Hofmann, R.; Muller, S. G.; Eckstein, R.; Hofmann, D. Determination of the Thermal Diffusivity and Conductivity of Mono-Crystalline Silicon Carbide (300 - 2300K), *High Temp. High Press.*, 1997, 29, 73 - 79.
- [67] NIST Property Data Summaries Data - Sintered Silicon Carbide (SiC) [Online] <http://www.ceramics.nist.gov/srd/summary/scdscs.htm> (Accessed 1st May 2015).
- [68] Sanchez-Lavega, A.; Salazar, A.; Ocariz, A.; Pottier, L.; Gomez, E.; Villar, L. M.; Macho, E. Thermal Diffusivity Measurements in Porous Ceramics by Photothermal Methods, *Appl. Phys. A.*, 1997, 65, 15 - 22.
- [69] Watari, K.; Nakano, H.; Sato, K.; Urabe, K.; Ishizaki, K.; Cao, S.; Mori, K. Effect of Grain Boundaries on Thermal Conductivities of Silicon Carbide Ceramic at 5 to 1300K, *J. Am. Ceram. Soc.*, 2003, 86[10], 1812 - 1814.
- [70] Hodgson, E. R.; Malo, M.; Manzano, J.; Morono, A.; Hernandez, T. Radiation Induced Modification of Electrical Conductivity for Three Types of SiC”, *J. Nucl. Mater.*, 2011, 417, 421 – 424.
- [71] Li, S.; Wang, N.; Zhao, H.; Du, L. Synthesis and Electrical Properties of P-Type 3C-SiC Nanowires, *Mater. Lett.*, 2014, 126, 217 - 219.
- [72] Kasahara, S.; Katano, Y.; Shimanuki, S.; Nakata, K.; Ohno, H. Electrical Conductivity Changes in Silicon Carbide under γ -Ray Irradiation, *J. Nucl. Mater.*, 1992, 191-194, 579 – 582.
- [73] Sun, J.; Li, J.; Sun, G.; Zhang, B.; Zhang, S.; Zhai, H. Dielectric and Infrared Properties of Silicon Carbide Nanopowders, *Ceram. Int.*, 2002, 28, 741 – 745.
- [74] Kim, K. J.; Lim, K. Y.; Kim, Y. W. Influence of Y_2O_3 Addition on Electrical Properties of β -SiC Ceramics Sintered in Nitrogen Atmosphere, *J. Eur. Ceram. Soc.*, 2012, 32, 4401 – 4406.
- [75] Sanchez-Gonzalez, J.; Ortiz, A. L.; Guiberteau, F.; Pascal, C. Complex Impedance Spectroscopy Studies of a Liquid Phase Sintered α -SiC Ceramic, *J. Eur. Ceram. Soc.*, 2007, 27, 3935 – 3939.
- [76] Hoffman, D.; Lely, J. A.; Volger, J. The Dielectric Constant of SiC, *Physica*, 1967, 23[1], 236.
- [77] Patrick L.; Choyke, W. J. Static Dielectric Constant of SiC, *Phys. Rev. B.*, 1970, 2, 2255.
- [78] Chauvet, O.; Solomon, I.; Zuppiroli, L. Electronic Properties of Disordered SiC Materials”, *Mat. Sci. and Eng.*, 1992, B11, 303 – 306.
- [79] Chauvert, O.; Stoto, T.; Zuppiroli, L. Hopping Conduction In A Nanometer-size Crystalline System: A SiC Fiber, *Phys. Rev. B.*, 1992, 46, 8139.
- [80] Su, X.; Zhou, W.; Li, Z.; Luo, F.; Du, H.; Zhu, D. Preparation and Dielectric Properties of B-Doped SiC Powder by Combustion Synthesis”, *Mat. Res. Bull.*, 2009, 44. 880 - 883.

- [81] Zhao, D. Zhao, H.; Zhou, W. Dielectric Properties of Nano Si/C/N Composite Powder and SiC powder at High Frequencies, *Physica E*, 2001, 9, 679 – 685.
- [82] Wereszczak, A. A.; Johanns, K. E.; Jadan, O. M. Hertzian Ring Crack Initiation in Hot Pressed Silicon Carbides, *J. Am. Ceram. Soc.*, 2009, 92[8], 1788 - 1795.
- [83] Sarva, S.; Nemat-Nasser, S. Dynamic Compressive Strength of Silicon Carbide under Uniaxial Compression, *Mater. Sci Eng.*, 2001, A317, 140 – 144.
- [84] Miyazaki, H.; Yoshizawa, Y.; Hirao, K. Fabrication of High Thermal-Conductive Silicon Nitride Ceramics with Low Dielectric Loss, *Mater. Sci. Eng. B*, 2009, 161, 198 - 201.
- [85] She, J.; Yang, J. F.; Jayaseelan, D. D.; Ueno, S.; Kondo, N.; Ohji, T.; Kanzaki, S. Strength of Silicon Nitride After Thermal Shock, *J. Am. Ceram. Soc.*, 2003, 86[9], 1619 – 1621.
- [86] Moulson, A. J.; Herbert, J. M. Electroceramics Materials· Properties· Applications, 2nd Ed.; John Wiley and Sons: West Sussex, UK, 2003; pp 269 – 289.
- [87] Chan, F.; Cao, F.; Pan, H.; Wang, K.; Shen, Q.; Shen, J.; Wang, S. Mechanical and Dielectric Properties of Silicon Nitride Ceramics with High And Hierarchical Porosity, *Mater. Des.*, 2012, 40, 562 - 566.
- [88] Othman, M. B. H.; Ramli, M. R.; Tyng, L. Y.; Ahmad, Z.; Akil, H. M. Dielectric Constant and Refractive Index of Poly-(Siloxane-Imide) Block Polymer, *Mater. Des.*, 2011, 32, 3173 – 3182.
- [89] Xia, Y.; Zeng Y. P.; Jiang, D. Mechanical and Dielectric Properties of Porous Si₃N₄ Ceramics Using PMMA as Pore Former, *Ceram. Intl.*, 2011, 37, 3775 -3779.
- [90] Yang, W.; Xie, Z.; Li, J.; Miao, H.; Zhang, L.; An, L. Ultra-Long single Crystalline α -Si₃N₄ Nano-wires: Derived from a Polymeric Precursor, *J. Am. Ceram. Soc.*, 2005, 88[6], 1647 – 1650.
- [91] Riley, F. L. Silicon Nitride and Related Materials”, *J. Am. Ceram. Soc.*, 2000, 83[2], 245 – 265.
- [92] Yao, D.; Xia, Y.; Zeng, Y. P.; Zuo K. H.; Jiang, D. Porous Si₃N₄ Ceramics Prepared via Slip Casting of Si and Reaction Bonded Silicon Nitride, *Ceram Int.*, 2011, 37, 3071 - 3076.
- [93] Xu, Z.; B. Wang, B.; Yang J.; Zhao, Z. Preparation of Porous Si₃N₄ Ceramics with Controlled Porosity and Microstructure by Fibrous α -Si₃N₄ Addition, *J. Am. Ceram. Soc.*, 2014, 91[11], 3392 – 3395.
- [94] Garcia-Moreno, O.; Fernandez, A.; Torrecillas, R. Conventional Sintering of LAS-SiC Nanocomposites with Low Thermal Expansion Coefficient, *J. Eur. Ceram. Soc.*, 2010, 30, 3219 – 3225.
- [95] Scheppokat, S.; Janssen, R.; Claussen, N. Phase Development and Shrinkage of Reaction-Bonded Mullite Composites with Silicon Carbide of Different Particle Sizes, *J. Am. Ceram. Soc.*, 1999, 82[2], 319 - 324.
- [96] Wu S.; Claussen, N. Fabrication and Properties of Low-Shrinkage Reaction-Bonded Mullite, *J. Am. Ceram. Soc.*, 1991, 74[10], 2460 - 2463.
- [97] Li, X.; Zhang, L.; Yin, X.; Yu, Z. Mechanical and Dielectric Properties of Porous Si₃N₄-SiC(BN) Ceramic, *J. Alloys. Compd.*, 2010, 490, L40 - L43.

- [98] Kobayashi, R.; Tatami, J.; Chen, I. W.; Wakihara, T.; Komeya, K.; Meguro, T.; Goto, T.; Tu, R. High Temperature Mechanical Properties of Dense AlN-SiC Ceramics Fabricated by Spark Plasma Sintering Without Sintering Additives, *J. Am. Ceram. Soc.*, 2011, 94[12], 4150 – 4153.
- [99] Gonzalez-Julian, J.; Milarzo, P.; Osendi, M. I.; Belmonte, M. Enhanced Tribological Performance of Silicon Nitride-Based Materials by Adding Carbon Nanotubes, *J. Am. Ceram. Soc.*, 2011, 94[8], 2542 – 2548.
- [100] Bodhak, S.; Bose, S.; Bandyopadhyay, A. Densification Study and Mechanical Properties of Microwave-Sintered Mullite and Mullite-Zirconia Composites, *J. Am. Ceram. Soc.*, 2011, 94[1], 32 - 41.
- [101] Gerhardt, R. A.; Ruh, R. Volume Fraction and Whisker Orientation Dependence of the Electrical Properties of SiC-Whisker-Reinforced Mullite Composites, *J. Am. Ceram. Soc.* 2001, 84[10] 2328 – 2334.
- [102] Singh, S.; Srivastava, V. K. Electrical Properties of C/C and C/C-SiC Ceramic Fiber Composites, *Ceram. Int.*, 2001, 37, 93 – 98.
- [103] Fa, L.; Huan, J.; Dongmei Z.; Wancheng, Z. Dielectric Properties of SiC/LAS Composite, *Mater. Lett.*, 2005, 59[1], 105 – 109.
- [104] Liu, H.; Tian, H. Mechanical and Microwave Dielectric Properties of SiCf/SiC Composites with BN Interphase prepared by Dip-Coating Process, *J. Eur. Ceram. Soc.*, 2012, 32, 2505 – 2512.
- [105] Kingery, W. D.; Bowen, H. K.; Uhlmann, D. R. *Introduction to Ceramics*, 2nd Ed.; John Wiley and Sons: New York, 1976; pp 448 - 517.
- [106] Rahaman, M. N.; *Ceramic Processing*, 2nd Ed.; CRC Press: Boca Raton, Florida, US, 2003, pp 1 - 30.
- [107] Evans, J. W.; De Jonghe, L. C. *The Production of Inorganic Materials*; Macmillian Publishing Co.: New York, 1991; 391 - 409.
- [108] Mcgreary, R. K. Mechanical Packing of Spherical Particles, *J. Am. Ceram. Soc.*, 1961, 44, 513 - 522.
- [109] Rahaman, M. N.; *Ceramic Processing*, 2nd Ed.; CRC Press: Boca Raton, Florida, US., 2003, pp 328 - 424.
- [110] Westman, A. E. R.; Hugill, H. R. The Packing of Particles, *J. Am. Ceram. Soc.*, 1930, 13[10], 767 – 779.
- [111] Lin, Y. J.; Tsang, C. P. Fabrication of Mullite/SiC and Mullite/Zirconia/SiC Composites by ‘Dual’ In-Situ Reaction Syntheses, *Mat. Sci. and Eng. A*, 2003, 344, 168 -74.
- [112] Leo, S.; Tallon, C.; Stone, N.; Franks, G. V. Near net Shaping Methods for Ceramic Elements of (Body) Armor Systems, *J. Am. Ceram. Soc.*, 2014, 97[10], 3013 – 3033.
- [113] Kim, D. K.; Kriven, W. M. Processing and Characterization of Multiphase Ceramic Composites Part I: Duplex Composites Formed in-Situ From Solutions, *J. Am. Ceram. Soc.*, 2008, 91[3], 784 - 792.
- [114] Pan, X.; Meyer, J.; M. Ruhle, M.; Niihara, K. Silicon Nitride Based Ceramic Nanocomposites, *J. Am. Ceram. Soc.*, 1996, 79[3], 585 - 590.
- [115] Niihara, K. J. New Design Concept of Structural Ceramics: Ceramic Nanocomposites, *J. Ceram. Soc. Jpn.*, 1992, 100[4], 536 – 540.
- [116] Lee, C. H.; Lu, H. H.; Wang, C. A.; Nayak, P. K.; Huang, J. L. Influence of Conductive Nano-TiC on Microstructural Evolution of Si₃N₄-based Nanocomposites in Spark Plasma Sintering, *J. Am. Ceram. Soc.*, 2011, 94[3], 959 -967.

- [117] Zheng, C. S.; Yan, Q. Z.; Xia, M.; Ge, C. C. In-situ Preparation of SiC/Si₃N₄-NW Composite Powder by Combustion Synthesis, *Ceram Int.*, 2012, 38, 487 -493.
- [118] Yang, W.; Zhang, L.; Xie, Z.; Li, J.; Miao, H.; An, L. Growth and Optical Properties of Ultra-Long Single Crystalline α -Si₃N₄ Nanobelts, *Appl. Phys A: Mater. Sci. Process.*, 2005, 80[7], 1419 – 1423.
- [119] Lee, M. Y.; Brannon, R. M.; Bronowski D. R. *Uniaxial and Triaxial Compression Tests of Silicon Carbide Ceramics under Quasi-static Loading Conditions*; SAND2004-6005; Sandia National Library (SNL), Albuquerque, NM, 2005.
- [120] Kikuchi, M. Effect of test Circumstances on Compressive Strength of Porous Calcium Phosphate Ceramics for Establishment of Standard Measurement Conditions, *Bioceramics Dev. Appl.*, 2011, 1, 1 - 3. (doi:10.4303/bda/D101201)
- [121] Moulson, A. J.; Herbert, J. M. *Electro-ceramics: Materials, Properties, Applications*, 2nd Ed., John Wiley and Sons: West Sussex, UK; 2003; pp 95 - 134.
- [122] Kingery, W. D.; Bowen H.K.; Uhlmann, D. R. *Introduction to Ceramics*, 2nd Ed., John Wiley and Sons Inc.: New York; 1976; pp 448 - 515.
- [123] Lin, C. C.; Zangvil, A.; Ruh, R. Modes of Oxidation in SiC-Reinforced Mullite/ZrO₂ Composites: Oxidation Vs Depth Behavior, *Acta Mater.*, 1999, 47[6], 1977 - 1986.
- [124] ASTM 773-88 (Reapproved 2006) – *Standard Test Method For Compressive (Crushing) Of Fired Whiteware Materials*; ASTM International: Pennsylvania, United States; 2006; pp 243 - 246.
- [125] Mensik, J. *Strength and Fracture of Glass and Ceramics*, Elsevier Science Publishing: Amsterdam, 1992; pp 163 - 164.
- [126] Lian, T. W; Kondo, A.; Akoshima, M.; Abe, H.; Ohmura, T.; Tuan W. H.; Naito, M. Rapid Thermal Conductivity Measurements of Porous Thermal Insulation Materials by Laser Flash Method, *Advanced Powder Technology*, 2016, (In Press).<http://dx.doi.org/10.1016/j.appt.2016.01.008>
- [127] Tsutsumi, N.; Takizawa, T.; Kiyotsukuri, T.; Thermal Diffusivity of Polymer by Flash Radiometry: Correlation Between Thermal diffusivity and Fine Structure of Poly(Ethylene Terephthalate), *Polymer*, 1990, 31, 1925 - 1931.
- [128] Twiss R. J.; Moore, E.M. *Structural Geology*, 2nd ed.; W.H. Freeman and Co.: New York, 2007; pp 459 - 494.
- [129] Brindley G. W.; Nakahira M. The Kaolinite-Mullite Reaction Series: I. A Survey of Outstanding Problems, *J. Am. Ceram. Soc.*, 1959, 42, 311 - 314.
- [130] Brindley G. W.; Nakahira M. The Kaolinite-Mullite Reaction Series: II. Metakaolin, *J. Am. Ceram. Soc.*, 1959, 42, 314 - 318.
- [131] Brindley G. W.; Nakahira M. The Kaolinite-Mullite Reaction Series: III. High Temperature Phases, *J. Am. Ceram. Soc.*, 1959, 42, 319 - 324.
- [132] Chandraborty, A. K. Formation of Silicon-Aluminum Spinel. *J. Am Ceram. Soc.*, 1979, 62 [3], 120 - 124.
- [133] Chakraborty, A. K; Ghosh, D. K. Comment on Spinel Phase Formation During 980°C Exothermic Reaction in the Kaolinite-to-Mullite Reaction Series, *J. Am Ceram. Soc.*, 1989, 72[8], 1569 - 1570.
- [134] Chen, C. Y.; Tuan W. H. Evolution of Mullite Texture on Firing Tape-Cast Kaolin Bodies, *J. Am Ceram. Soc.* 2002, 85[5], 1121 - 1126

- [135] Yang, K. H.; Wu, J. H.; Hsi, C. S.; Lu, H. Y. Morphologically Texture Mullite in Sintered Tape-Cast Kaolin. *J. Am Ceram. Soc.*, 2011, 94[3], 938 - 944.
- [136] Dong, L.; Zhang, C.; Chen, Y. J.; Cao, L. H.; Li, J. B.; Luo, L. J. Acicular Porous Mullite From Diatom Frustules, *Mater. Lett.*, 2016, 171, 108 – 111.
- [137] Hsiung, C. H. H.; Pyzik, A. J.; De Carlo, F.; Xiao, X.; Stock, S. R.; Faber, K. T. Microstructure and Mechanical Properties of Acicular Mullite, *J. Eur. Ceram. Soc.*, 2013, 33, 503 – 513.
- [138] Grimshaw, R. W. The Chemistry and Physics Clays and Allied Ceramic Materials', 4th Ed., Ernest Benn Ltd.: London, UK; 1971; pp 430.
- [139] Zhao, J. Z., Liu, Z. L.; Li, Y. M. Preparation and Characterization of Low-Density Mullite-Based Ceramic Proppant by A Dynamic Sintering Method., *Mater. Lett.*, 2015, 152, 72 – 75.
- [140] Kanka, B.; Schneider, H. Sintering Mechanisms and Microstructural Development of Co-precipitated Mullite, *J. Mater. Sci.*, 1994, 29, 1239 – 1349.
- [141] Fan, Z.; Tsakiroopoulos, P; Miodownik, A. P. A Generalized Law of Mixtures, *J. Mater Sci.*, 1994, 29, 141 - 150.
- [142] Kingery, W. D., Bowen, H. K.; Uhlmann, D. R. Introduction to Ceramics, John Wiley & Sons: New York; 1976; pp 485.
- [143] Liu, D. M. Thermal Diffusivity of Porous $(\text{Ca}_{1-x}\text{Mg}_x)\text{Zr}_4(\text{PO}_4)_6$ Ceramic, *Mater. Chem. Phys.*, 1994, 36, 350 - 353.
- [144] Bari, K.; Osarinmwian, C.; Lopez-Honorato, E.; Abram, T. J. Characterization of the Porosity in TRISO Coated Fuel Particles and Its Effect on the Relative Thermal Diffusivity. *Nucl. Eng. Des.*, 2014, 265, 668 – 674.
- [145] Brinkman, C. R.; Quinn, G. D. Chapter 8: Standardization of Mechanical Properties Tests for Advanced Ceramics. In *Mechanical Testing and Methodology for Ceramic Design and Reliability*; Cranmer D. C.; Richerson, D. W. eds.; Marcel Dekker Inc.: New York, 1998; pp 353 - 386.
- [146] Twiss R. J.; Moore, E. M. *Structural Geology*, 2nd ed.; W.H. Freeman and Co.: New York, 2007; pp 209 - 230.
- [147] Schneider, H.; Chapter 2: Basic Properties of Mullite; 2.1.3: Microhardness of Mullite. In *Mullite*; Schneider, H.; Komarneni, S. eds; Wiley VCH GmbH: Weinheim, Germany; 2005; pp 146 - 148.
- [148] Ismail, M. G. M. U.; Nakai Z.; Somiya, S. Microstructure and Mechanical Properties of Mullite Prepared by the Sol-Gel Method, *J. Am. Ceram. Soc.*, 1987, 70, C7 - C8.
- [149] Kelly, W. H.; Palazotto, A. N.; Ruh, R.; Heuer J. K.; Zangoil, A.; Thermal Shock Resistance of Mullite and Mullite-ZrO₂-SiC Whiskers Composites, *Ceram. Eng. Soc. Proc.*, 1997, 18, 195 – 203.
- [150] Wu S.; Claussen, N. Reaction Bonding and Mechanical Properties of Mullite/Silicon Carbide Composites, *J. Am. Ceram. Soc.*, 1994, 77[11], 2898 -2904.
- [151] Sawaguchi, A.; Toda K.; Niihara, K. Mechanical Properties of Silicon Nitride-Silicon Carbide Nanocomposite Materials, *J. Am. Ceram. Soc.*, 1991, 74[5], 1142 - 1144.

- [152] McCabe J. F.; Walls, A. W. G. Properties Used to Characterize Materials: 2.2 Mechanical Properties. In *Applied Dental Materials*, 9th Ed., Blackwell Publishing: Oxford, UK; 2008, [Online] <http://download.e-bookshelf.de/download/0003/7903/64/L-X-0003790364-0002227810.XHTML/index.xhtml> (accessed on 3rd May 2015).
- [153] Ceramics Society of Japan (eds.), *Handbook of Ceramics: Volume 1* 2nd Ed., Gihodo Publishing: Tokyo, 2002; pp 313 - 314.
- [154] Ceramics Society of Japan (eds.), *Handbook of Ceramics: Volume 1*; 2nd Ed., Gihodo Publishing: Tokyo, 2002; pp 1249 - 1250.
- [155] Pitchford, J. E.; Stearns, R. J.; Kelly, A.; Clegg, W. J. Effects of Oxygen Vacancies on the Hot Hardness of Mullite, *J. Am. Ceram. Soc.*, 2001, 84, 1167 - 1168.
- [156] Schneider, H.; Basic Properties of Mullite; 2.1.2: Elastic Moduli and Compressibility (of Mullite). In *Mullite*; Schneider, H.; Komarneni, S.eds; Wiley VCH : Weinheim, Germany, 2005; pp 142 - 145.
- [157] Mensik, J. *Strength and Fracture of Glass and Ceramics*, Elsevier Science Publishing: Amsterdam, 1992; pp 20 - 23.
- [158] Mensik, J. *Strength and Fracture of Glass and Ceramics*, Elsevier Science Publishing: Amsterdam, 1992; pp 73 -76.
- [159] Mensik, J. *Strength and Fracture of Glass and Ceramics*, Elsevier Science Publishing: Amsterdam, 1992; pp 163 - 164.
- [160] Yonezu, A.; Hirayama, K.; Kishida, H.; Chen, X. Characterization of The Compressive Deformation Behavior with Strain Rate Effect of Low-Density Polymeric Foams, *Polymer Testing*, 2016, 50, 1 – 8.
- [161] Jiang, B.; Zhao, Q.; He, C.; Shi, C.; Zhao, N. A Novel Method for Synthesizing Ultralight Silver Foams by the Silver Mirror Reaction, *Mater. Lett.*, 2016, 173, 80 – 83.
- [162] Jonscher, A. K. “Chapter 1” in *Dielectric Relaxation in Solids*, Chelsea Dielectric Press, London, UK, 1983, pp 22 – 33.
- [163] Chandraborty A. K.; Ghosh, D. K.; Reexamination of the Kaolinite-to-Mullite Reaction Series, *J. Am. Ceram. Soc.*, 1978, 61[3-4], 170 – 173.
- [164] Schonhals, A.; Kremer, F.; Chapter 3: Analysis of Dielectric Spectra – Separation of Charges. In *Broadband Dielectric Spectroscopy*; Kremer F.; Schonhals, A., Eds; Springer Verlag: Berlin, Germany, 2003, pp 87 – 90.
- [165] Jonscher, A. K. Dielectric Characterization of Semiconductors, *Solid State Electron*, 1990,. 33[6], 737 – 740.
- [166] Kabir, M. F. ; Daud, W. M.; Khalid K. B.; Sidek, A. H. A. Equivalent Circuit Modeling of the Dielectric Properties of Rubber Wood at Low Frequency, *Wood Fiber Sci.*, 2000,. 32[4], 450 – 457.
- [167] King, S. W.; Bielefeld, J.; French M.; Lanford, W. A. Mass and Bond Density Measurement for PECVD α -SiC_x:H Thin Films Using Fourier Transform-Infrared Spectroscopy, *J. Non-Cryst. Solids*, 2011, 357, 3602 – 3615.
- [168] Zheng, G.; Yin, X.; Wang, J.; Guo M.; Wang, X.; Complex Permittivity and Microwave Absorbing Property of Si₃N₄-SiC Composite Ceramic, *J. Mater. Sci. Technol.*, 2012, 28[8], 745 – 750.
- [169] Knotek, M. L.; Pollak, M.; Correlation Effects in Hopping Conduction: Hopping as a Multi-Electron Transition, *J. Non-Cryst. Solids*, 1972, 8[10], 505 – 510.

- [170] Wang, S.; Jia, D.; Yang, Z.; Duan, X.; Tian, Z.; Zhou, Y. Effect of BN Content on Microstructures, Mechanical and Dielectric Properties of Porous BN/Si₃N₄ Composite Ceramics Prepared by Gel Casting, *Ceram. Int.*, 2013, 39, 4231 – 4237.
- [171] Rahaman, M. N.; Yao, A.; Bal, B. S.; Garino, J. P.; Ries M. D. Ceramics for Prosthetic Hip and Knee Joint Replacement, *J. Am. Ceram. Soc.*, 2007, 90[7], 1965 - 1988.
- [172] Aksay, I. A.; Dobbs, D. M.; Sarikaya, M. Mullite for Structural, Electronics and Optical Applications, *J. Am. Ceram. Soc.*, 1991, 74[10], 2343 – 2358.

